

On-device modeling of user’s social context and familiar places from smartphone-embedded sensor data

Mattia G. Campana^{a,*}, Franca Delmastro^a

^a*Institute for Informatics and Telematics of the National Research Council of Italy (IIT-CNR), Via Giuseppe Moruzzi, 1 56124 Pisa, Italy*

Abstract

Context modeling and recognition represent complex tasks that allow mobile and ubiquitous computing applications to adapt to the user’s situation. The real advantage of context-awareness in mobile environments mainly relies on the prompt system’s and applications’ reaction to context changes. Current solutions mainly focus on limited context information generally processed on centralized architectures, potentially exposing users’ personal data to privacy leakage, and missing personalization features. For these reasons on-device context modeling and recognition represent the current research trend in this area. Among the different information characterizing the user’s context in mobile environments, social interactions and visited locations remarkably contribute to the characterization of daily life scenarios. In this paper we propose a novel, unsupervised and lightweight approach to model the user’s social context and her locations based on *ego networks* directly on the user mobile device. Relying on this model, the system is able to extract high-level and semantic-rich context features from smartphone-embedded sensors data. Specifically, for the social context it exploits data related to both physical and cyber social interactions among users and their devices. As far as location context is concerned, we assume that it is more relevant to model the familiarity degree of a specific location for the user’s context than the raw location data, both in terms of GPS coordinates and proximity devices. We demonstrate the effectiveness of the proposed approach with 3 different sets of experiments by using 5 real-world datasets collected from a total of 956 personal mobile devices. Specifically, we assess the structure of the social and location ego networks, we provide a semantic evaluation of the proposed models and a complexity evaluation in terms of mobile computing performance. Finally, we demonstrate the relevance of the extracted features by showing the performance of 3 different machine learning algorithms to recognize daily-life situations, obtaining an improvement of 3% of AUROC, 9% of Precision, and 5% in terms of Recall with respect to use only features related to physical context.

*Corresponding author

Email addresses: m.campana@iit.cnr.it (Mattia G. Campana),
f.delmastro@iit.cnr.it (Franca Delmastro)

Keywords: context-recognition; social-context; ego networks; feature extraction; mobile sensing; on-device machine learning

1. Introduction

The increasing computational and sensing capabilities of mobile devices, along with their pervasiveness in our daily lives, have contributed to the rapid expansion and evolution of the Internet at its edges [1]. Specifically, mobile systems do not represent only the data collection point for a subsequent centralized elaboration, but they are becoming the core of the data modeling and processing, by exploiting on-device computation capabilities [2, 3]. This new paradigm creates additional opportunities for the development of novel pervasive and context-aware mobile applications which can benefit from low-latency device-to-device communications and sensing capabilities of modern mobile devices. Examples of these applications include networking services, like data dissemination algorithms [4] and forwarding protocols [5], but also application-oriented services like mobile health systems [6, 7], intelligent transportation systems [8], augmented reality applications [9], and pervasive recommender systems [10, 11].

Context-awareness represents the key feature of such applications. Specifically, the great variety of sensors embedded in modern mobile devices (e.g., smartphones and wearables) provides essential information to recognize different aspects of the user's daily life, including, for example, movements and body postures [12] and daily life situations [13]. According to Rawassizadeh et al. [3], processing user's data directly on the local device provides several advantages. Firstly, it allows both the device and the applications to quickly adapt their behavior according to the user's situation and needs. Since the mobile environment can be particularly dynamic, the application scenario in which the device is employed might rapidly change according to our daily activities. Secondly, user privacy can considerably benefit from the use of such a decentralized approach [14]. In fact, traditional client-server solutions may demotivate privacy-aware people to use pervasive applications since a third-party entity will be in charge of storing and processing their data, thus requiring additional mechanisms to safeguard their privacy [15]. On the contrary, shifting the computation from remote servers to the user device allows the system to preserve her privacy, avoiding trusting external entities. In the last few years, such advantages have been found in several application domains, including IoT [16], healthcare [17], and smart-cities [18], thus highlighting the need for a paradigm change. Finally, on-device analysis has been proven to be more energy-efficient than offloading the data processing to remote infrastructures, especially when the size of the data grows [19].

Among the possible context information, social relationships and location are two of the most relevant features proposed in the literature to model the user's context in mobile environments [20, 21]. They can be particularly effective not just to recognize the user's daily activities, but also to characterize her

preferences and needs based on the place she is currently visiting and with whom. However, existing solutions to extract such information from user’s data strongly rely on a centralized approach. Social relationships among users are typically modeled from a global point of view, analyzing a big amount of data collected through crowd-sensing techniques to identify, for example, communities of users with similar interests or behaviors [22]. On the other hand, the user’s location is usually characterized by labels associated with geographical coordinates on centralized databases (e.g., Foursquare ¹ and Google Places ²). Such approaches mainly provide general-purpose results without taking into account the individual characteristics and needs of the single user. Instead, it would be really useful to associate to a location or a person the familiarity degree of the local user. This would provide a personalized evaluation of the social and location contexts that could further optimize the final application.

In order to fill this gap, in this paper we investigate the use of the *ego network* model to characterize both the user’s *social context* and *location information* as an efficient, unsupervised, and lightweight approach to mine high-level and semantic-rich context features derived from smartphone-embedded sensor data, by performing the entire processing on the mobile device. An ego network is a special type of graph with a star topology that typically describes the relationships between an individual (*ego*) and its peers (*alters*) [23], in which the alters are organized in a hierarchical structure based on their interaction frequencies with the ego. Such a characteristic makes the ego network a simple but effective tool to automatically discriminate between relevant and casual ego-alter links, without requiring a learning phase or fixing thresholds during the system design. To the best of the authors’ knowledge, this is the first time ego networks are used to model both the user’s social context and her visited locations in mobile and distributed computing.

Another important difference with existing solutions is the type of data used to define these models. In this case social context and location information are based on data derived from smartphone-embedded sensors and from the user interaction with her personal mobile device. As shown in Figure 1, we envision the implementation of the proposed models as part of a pre-existing middleware architecture [13], which includes all the necessary components to perform the context-recognition task directly on the user’s device: a Sensing Manager (SM) layer that unobtrusively collects context data from both physical and virtual sensors available on mobile devices, a Context Modeling (CM) layer aimed at processing raw sensor data to extract meaningful features to characterize the user’s context; and a Context Reasoning (CR) layer that relies on such features to recognize the user’s context by using machine learning models, including both unsupervised clustering solutions [24, 25] and pre-trained supervised classifiers (e.g., Random Forest and Artificial Neural Networks [26, 27]).

Specifically, we propose the *Social Context* and *Familiar Places* modules

¹<https://developer.foursquare.com>

²<https://developers.google.com/maps>

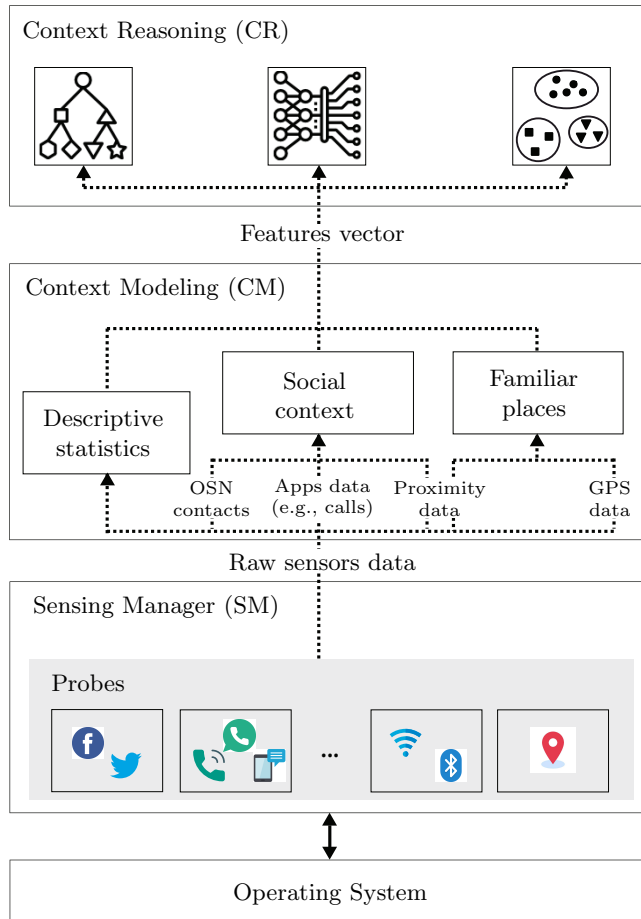


Figure 1: High-level architecture of the context-aware middleware solution implementing the proposed algorithms to model the user’s social context and familiar places based on heterogeneous sensors data.

that are especially designed to be executed online on the mobile device and automatically updated when new data is available. The Social Context component models the user’s social relationships by creating an ego network based on heterogeneous social signals, including applications data (e.g., calls and messages), face-to-face interactions, and activities performed on Online Social Network platforms (OSN). The underlying idea of combining such heterogeneous data sources has its origin in the *cyber-physical convergence theory*: according to Conti et al. [28], mobile devices act as gateways between the physical world around us and the virtual world of the Internet, making them deeply interwoven, constantly interacting with each other. However, previous works on ego networks only focus on one dimension of the user’s social context, modeling her social relationships either offline [29] or online [30], mainly trying to demonstrate

the correspondence between physical and virtual social relationships. On the contrary, in our case the idea is to create a unified model that combines both dimensions, thus characterizing different aspects of the user’s social context while using the mobile technology.

To be effective, the Social Context module must be able to identify the alters in the social signals collected by SM. To this aim, each user must be associated with unique identifiers, such as her OSN ID, phone number, and MAC addresses of the available wireless interfaces of her mobile device. This can be achieved by using a fully-distributed approach, allowing the mobile devices to share the required information among them through the use of device-to-device (D2D) communication channels. This implies specific procedures to ensure both the compliance with the user’s privacy management and the secure communication of personal information. Specifically, the user’s identifiers can be encrypted by the middleware and shared with other devices in proximity by using the available D2D technologies, such as Wi-Fi Direct (WFD) and Bluetooth LE (BLE) Services [31, 32]. Upper layer applications do not need the access to this information, and the middleware can maintain only the encrypted identifier in order to guarantee pseudo-anonymization. In this way, through a fully distributed approach the user maintain a local control on her personal data, finely selecting which information to share through the middleware settings.

Similar to the Social Context module, the Familiar Places component relies on the ego networks to model the level of familiarity of the user’s locations based on their visiting frequencies. For example, the user’s home and workplace could be the locations in which she spends the majority of her daily time, while occasionally visited locations might represent specific shops or restaurants. This module creates two distinct ego networks where the alters represent GPS locations and smart devices in proximity, respectively. Creating specific models for different location data sources allows the Familiar Places module to analyze the user’s location from two distinct perspectives. On the one hand, the GPS-based ego network aims at characterizing outdoor places, where the GPS signal is typically high enough to accurately identify her geographical location. On the other hand, when the user is located inside a building, the proximity-based model is crucial to characterize the nearby environment by creating a sort of fingerprint of the place based on the wireless-enabled smart devices available in the nearby (e.g., Wi-Fi Access Points, printers, and home personal assistants). In this way, our approach is able to automatically identify the most familiar places of the user, extracting semantic-rich features without relying on external services.

To validate the proposed approach, we firstly analyze the structure of the Social Context and Familiar Places ego networks by using 5 real-world datasets collected by a total of 956 personal mobile devices. We also assess the ability of both modules to extract semantic-rich features by using the Ground Truth contained in 3 of the considered datasets. Then, we provide a complexity analysis aimed at demonstrating the feasibility of the models’ execution on resource-constrained devices. Finally, as a proof-of-concept application, we show how the extracted features can be used to improve the recognition of daily-life activities

based on smartphone-embedded sensor data and machine learning classifiers.

In summary, the paper provides the following contributions:

- The introduction of ego networks in mobile context modeling demonstrating their efficacy to extract semantic-rich features from mobile sensor data describing social context and location information.
- The experimental evaluation of the effectiveness of the proposed solutions on 5 public datasets collected from real mobile devices.
- A theoretical and empirical evaluation of the time complexity of the execution of the proposed models on resource-constrained devices.
- A real application scenario in which the extracted features improve the performance of 3 machine learning classifiers commonly used for context-recognition to identify daily-life activities from smartphone sensors data.

The remainder of the paper is organized as follows. In Section 2, we present the related works referring to both mobile sensors features extraction and ego networks applications. Section 3 presents the proposed models for Social Context and Familiar Places. Section 4 outlines the experimental settings used to validate the proposed solutions and discusses the obtained results. Section 5 describes the models' complexity evaluation to demonstrate their mobile computing performances. Then, in Section 6, we present a use-case scenario demonstrating the performance of machine learning classifiers in recognizing the user's context based on the selected sensor data. Eventually, in Section 7, we draw our conclusions and present some directions for future works.

2. Related work

The novel contributions of this paper with respect to the state of the art include multiple aspects. First of all, it introduces a new way to analyze mobile sensor data, both physical and virtual, and extract relevant features to characterize the social context of a user and her visited locations. In addition, it presents the first attempt to use ego networks to extract those features. For these reasons, this section will briefly discuss the state of the art both in sensing data analysis for context recognition and ego networks modeling.

As far as sensing data analysis is concerned, most of the previous works mainly focus on human activity recognition. In those cases, raw sensors data is firstly processed to extract descriptive statistics that characterize the current user's activity, including average value, absolute difference, time between peaks, and distribution's skewness. Then, those features are commonly used as input to machine learning classifiers to infer high-level semantics from data. For example, Voicu et al. [33] used three motion sensors commonly available on smartphones (i.e., accelerometer, gyroscope, and gravity sensor) to recognize different labels related to the user's gait (e.g., *walking*, *running*, and *sitting*), while Zebin et al. [27] recognized similar activities by using wearable inertial sensors and a deep

learning model. Moreover, physical sensors are also broadly used to identify transportation modalities (e.g., *walk*, *run*, *bike*, *bus*, and *train*) [34, 35], and to characterize different well-being and health conditions of the user, including sleep quality [36] and stress level [37].

However, the user’s context in mobile environments refers to more complex activities describing, for example, daily life situations as *working*, *shopping*, or *watching a movie with friends*. Modeling such contexts requires the fusion of a heterogeneous and broad set of data extracted from not just physical sensors, but also virtual sensors characterizing the interactions between the user and her device, and the surrounding environment including, for example, the list of running applications, the device hardware status, and the list of other devices in the nearby. Recently, only a few researchers have investigated the use of high-dimensional data to recognize daily activities and behavioral patterns [38]. For instance, Vaizman et al. [39] proposed a multi-layer perceptron to recognize daily-life situations (e.g., *At home*, *Cooking*, and *Computer work*) based on the fusion of different context signals collected from both smartphones and wearable devices, including motion sensors, phone state (e.g., running application and Wi-Fi connectivity), audio recordings, and the user’s GPS coordinates. On the other hand, other researchers combine such information with data collected from external sensors available in the nearby to detect human behaviors in smart environments [40, 41].

Social context, in terms of interpersonal relationships with other users, has been underestimated by previous works in shaping the user’s daily activities, even though it has been proved in the literature that there is a strong correlation between human activities and social data [42]. In fact, modeling the user’s personal network of social relationships can greatly contribute to highlight the differences among the contexts in which she can be involved in mobile scenarios (e.g., working with colleagues, or chatting with friends). To this aim, social networks analysis can be performed at the (i) *macroscopic* level, which investigates the global properties of the whole structure of social networks, and at the (ii) *microscopic* level, that aims at characterizing the social networks of single individuals, taking into account only the portion of the network composed by the set of relationships of a particular user [43]. Since we are interested in modeling the user’s social context in mobile environments, we mainly focus on the latter one, with particular reference to the use of *ego networks* [44].

According to the sociological theory postulated by Roberts and Dunbar [45, 46], the social ties of an ego network do not have the same relevance. Each individual has only a few strong links and many more weak ties, due to the limited human cognitive capacity to handle too many social relationships [47]. A visual representation of the ego network structure is shown in Figure 2: the ego is placed at the center of four or five concentric circles (also called *layers*) in which the alters are distributed according to the strength of their social ties with the ego. The innermost circle (*support clique*) is the smaller layer, containing only a few alters representing the strongest social relationships of the ego. The second layer (*sympathy group*) contains those people that can be considered as close friends. The third circle (*affinity group*) is composed by casual friends and

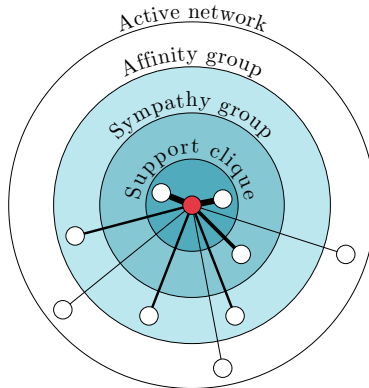


Figure 2: Structure of an ego network. The red circle in the center represents the *ego*, while the white ones are the *alters*. The links between the ego and its alters are depicted based on their strength: thicker is the line and stronger is the relationship between the ego and the specific alter.

extended family members, while the last layer (*active network*) includes people with whom the individual has occasional social interactions. The ego network model has been successfully used to characterize the social relationships in both OSN platforms, like Facebook and Twitter [30, 48], and offline social networks, based on surveys [49], phone call logs [29], and Bluetooth proximity [50]. However, to the best of our knowledge, their application to model social relationships in a combination of the two worlds has not yet been explored.

As far as location information is concerned, its use as context information has been well investigated to facilitate the provisioning of personalized services, including location-based marketing, social networking, and recommendations [51, 52]. For example, Do and Gatica-Perez [53] presented a framework for predicting future user’s location and which mobile applications she will use by exploiting different contextual information from smartphone sensors, including the user’s locations history. On the other hand, Niu et al. [54] have recently proposed a clustering-based approach to discover significant places for the mobile user by analyzing her spatial and temporal trajectories. Even though current solutions are effective in mining meaningful information from raw GPS traces, they are ultimately based on centralized approaches, where a big amount of data are processed by using offline techniques. Moreover, grouping GPS coordinates in clusters is effective to attenuate the approximation error introduced by the positioning system available on commercial mobile devices, but this approach is inadequate to discriminate between relevant and casual locations for the user. To this aim, in this work, we propose the use of ego networks as an unsupervised and online model to effectively characterize the user’s location by extracting valuable information from mobile sensors data by taking into account her behavior and habits. In the last few years, several works propose to use ego networks to study a broad set of phenomenons, including human migrations [55, 56], transportation modalities [57], language production [58], and

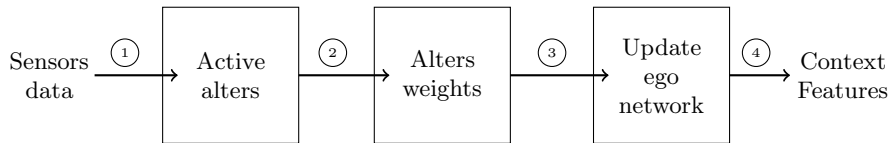


Figure 3: Modeling process implemented by both the Social Context and Familiar Places modules.

texts classification [59], but they have never been used to model user’s context information directly on mobile devices. Leveraging a similar methodology, we introduce the concept of *ego network of locations* to automatically recognize the level of familiarity of the venues visited by the mobile user by performing the entire data processing on the local device.

3. Modeling the user’s social context and familiar locations

The modeling process implemented by both the Social Context and Familiar Locations modules is graphically represented in Figure 3, which can be summarized in the following 4 main steps:

1. Sensor data is processed to identify the so-called *active-alters*, which, in our case, represent either other people with whom the local user is interacting with, or visited locations;
2. for each active alter, a relevance weight is computed, based on its past interactions with the ego (i.e., social interactions or visits);
3. the ego-network model is updated to reflect the changes in the user’s social relationships and her familiar locations, by possibly re-organizing the alters among its layers based on the new computed weights;
4. the active alters are classified according to their position in the ego-network, and a set of features is generated to characterize the user’s social context and her location.

In the following sections we present the details of both the modules, describing how the alters’ weights are computed and how the ego networks are dynamically updated as soon as new context data is available from the underlying sensors. Moreover, Table 1 describes the main notation used to define the proposed models.

3.1. The Social Context module

The Social Context module characterizes the user’s social relationships relying on the typical hierarchical structure of the social ego networks model, but exploiting both physical and cyber interactions. On the one hand, OSN represent an invaluable source of social data to characterize the user’s virtual social relationships. *On the other hand, sensing information including proximity data and phone calls/SMS logs (or, more generally, messaging applications logs) are*

Table 1: Notation used in the definition of the Social Context and Familiar Places modules. Here, e indicates the *ego* (i.e., the local user), while a represents an alter.

Scope	Symbol	Description
Social Context	$\omega_v(e, a)$	virtual social weight between e and a
	$\omega_p(e, a)$	physical social weight between e and a
	$\omega_s(e, a)$	overall social weight between e and a
	\mathcal{S}_v	set of OSN data sources
	\mathcal{S}_p	set of physical social data sources
Familiar Places	$I_s(e, a)$	number of social interactions between e and a for the data source s
	$\omega_l(a)$	proximity-based weight of a
	n_a	number of times a has been in proximity of e
	Δ_{t_1, t_2}	difference between the timestamps t_1 and t_2

essential to model social interactions in the real life. For this reason, we decided to model the users social interactions by using the following data sources: (i) phone calls and SMS logs, (ii) proximity data, and (iii) activities performed by the user on OSN platforms.

The first step to build the ego network of an individual is to estimate the strength of the social ties with its alters. In this regard, several studies have highlighted that the number of interactions between two subjects is a valid indicator of the strength of their social relationship [60]. Based on this consideration, to model the strength of the user’s social ties in the cyberspace, we take into account different activities performed by the users on OSN, including *comments*, *reactions* (e.g., likes) and people *mentioned* (i.e., tagged) in her shared contents. Formally, the strength of the virtual social link between the ego e and an alter a , $\omega_v(e, a)$, is calculated as follows:

$$\omega_v(e, a) = \sum_{s \in \mathcal{S}_v} I_s(e, a), \quad (1)$$

where \mathcal{S}_v is the set of the aforementioned OSN data sources, and the function $I_s(e, a)$ calculates the number of interactions between e and a for a given data source $s \in \mathcal{S}_v$.

On the other hand, to characterize the user’s physical social links we calculate the number of interactions with other people based on mobile applications, including also *phone calls* and *SMS* logs, and *face-to-face contacts* inferred by using wireless communication technologies. Specifically, we consider both Bluetooth/ Bluetooth-LE (BT) and Wi-Fi Direct (WFD) scan data related to personal mobile devices of other people that are close enough to suppose to have a social interaction with the local user. To this aim, the Social Context module firstly filters out data related to devices with a signal strength (RSSI) less than -65 dBm. According to the literature [61], such a RSSI threshold allows us to take into account only those proximity data that represent face-to-face interac-

tions among the users, both in indoor and outdoor scenarios. However, wireless scans can be noisy since the local user might be in proximity of wireless-enabled but not personal devices, such as smart TVs, printers, smart bulbs, and home assistant devices (e.g., Amazon Alexa and Google Home). Therefore, we finally select only personal mobile devices (e.g., smartphones and wearables) based on their functionalities information provided by the respective wireless technologies, that is, the *Bluetooth Class ID* ³ for BT, and information shared through *Wi-Fi Direct Services* (i.e., UPnP ⁴ and Bonjour ⁵ networking protocols) for WFD.

Similarly to the virtual social links, we define the strength of the physical social relationship between the ego e and an alter a , $\omega_p(e, a)$, as the number of their interactions through mobile apps (including phone calls and SMS), and physical proximity as follows:

$$\omega_p(e, a) = \sum_{s \in \mathcal{S}_p} I_s(e, a), \quad (2)$$

where \mathcal{S}_p is the set of considered physical data sources, and $I_s(e, a)$ represents the number of interactions between the two users for the given data source, e.g., the number of times they had a phone call, or a face-to-face contact. Finally, the overall strength of the social link between e and a is given by the linear combination of the previous weights as follows:

$$\omega_s(e, a) = \lambda \cdot \omega_v(e, a) + (1 - \lambda) \cdot \omega_p(e, a), \quad (3)$$

with a parameter λ governing the relative importance of the virtual and social interactions, respectively.

Such a simple definition of the alters' weights allows our solution to quickly process the sensors data directly on the mobile device, updating the model as soon as the user's context changes. Indeed, every time new social data is available, the Social Context module firstly extracts the list of users with whom the local user is interacting with, called *active alters*. Then, for each active alter, the corresponding social weight is computed according with Equation 3. Please note that, for this step, the full history of past interactions between the local user and her alters is not required. On the contrary, for each alter, the Social Context module keeps in memory only the last computed weight, which is incrementally updated as soon as new social interactions are identified.

Once the social weights of the active alters have been computed, the user's social ego network can be dynamically updated by using Algorithm 1, which requires as input the following 5 arguments: (i) $\mathcal{A} = [w_1, w_2, \dots, w_n]$, the ranking of previously computed alters' weights sorted in descending order; (ii) $\mathcal{W} = [w_{a1}, w_{a2}, \dots, w_{an}]$, the active alters' weights; (iii) \mathcal{E} , the current ego network model; l , the number of layers of the ego network, and η , a parameter

³<https://www.bluetooth.com/specifications/assigned-numbers/baseband>

⁴<https://openconnectivity.org/developer/specifications/upnp-resources/upnp>

⁵<https://developer.apple.com/bonjour>

Algorithm 1 Ego Network dynamic update

```
1: Input
2:    $\mathcal{A}$  ranking of the alters' weights (descending order)
3:    $\mathcal{W}$  active alters' weights
4:    $\mathcal{E}$  current ego network
5:    $l$  number of layers
6:    $\eta$  maximum number of alters to keep in  $\mathcal{E}$ 
7: function UPDATEEGONET( $\mathcal{A}, \mathcal{W}, \mathcal{E}, l, \eta$ )
8:    $\mathcal{A}' \leftarrow \mathcal{A} \cup \mathcal{W}$  ▷ Update  $\mathcal{A}$  with the new weights
9:   if  $\mathcal{A}'_\eta \neq \mathcal{A}_\eta$  then ▷  $\mathcal{A}_\eta =$  first  $\eta$  elements in  $\mathcal{A}$ 
10:     $\mathcal{E} \leftarrow HC(\mathcal{A}'_\eta, l)$  ▷ Hierarchical Clustering in  $l$  layers
11:  end if
12:   $\mathcal{A} \leftarrow \mathcal{A}'$ 
13:  return  $\mathcal{E}$ 
14: end function
```

that indicates the maximum number of alters to use to build the social ego network. The algorithm firstly updates the alters' weights ranking with those of the active alters. Then, only if the new weights modify the first η positions of \mathcal{A} , the ego network model must be re-calculated because the user's social relationships might be changed since the last update. To this aim, the first η weights are clustered by using the Hierarchical Clustering approach [62], which produces as output the layered structure of the user's ego network, where the innermost circles host the alters with whom the user has social interactions more frequently (e.g., close friends and colleagues), while occasional interactions (e.g., acquaintances) are located in the outer circles. In other words, the parameter η is required to keep the model accurate and its update as fast as possible, taking into account only the most relevant interactions between the ego and her alters.

The presence of the threshold η finds its ground reason in the anthropological literature. In fact, according to the *social brain hypothesis* developed by Dunbar [63] and verified in several experiments [64, 65], to model the user's social relationships, η can be surely set to 150, which represents the human cognitive limit to the number of people with whom an individual can maintain stable social relationships. Such characteristic allows the model to dynamically keep track of the changes in the structure of the user's social relationships. The more the ego interacts with an alter a , the more a will rise in the ranking, thus becoming part of her ego network. On the contrary, when the interactions between the ego and a become less frequent, the alter will be gradually moved to the outer circles of the network, until it completely leaves the social network when its position in the ego's ranking overtakes the threshold *eta*.

Once the model is updated, the active alters can be finally classified based on the layers of the user's ego network in which they are located. At a given time t , the final output of the Social Context module is an array $SC_t = [aa_1, aa_2, \dots, aa_l]$, where each element, aa_i , represents the percentage of ac-

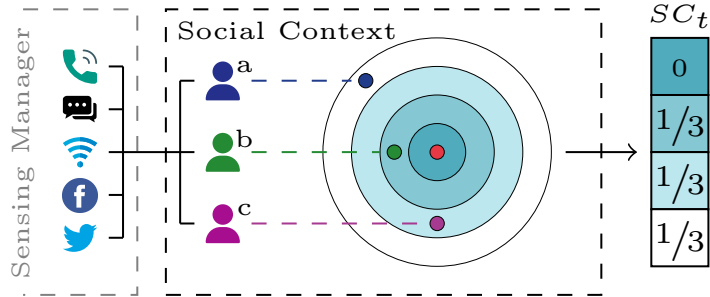


Figure 4: Recognition of the user’s social context. People interacting with the local user (called active alters) are extracted from the social data sources available in the Sensing Manager and they are classified by using the ego network model based on the past interactions. The output generated by the Social Context module at a given time t , SC_t , represents the percentage of active alters in each layer.

tive alters in each of the l layers that compose the user’s ego network, thus describing the user’s social context in terms of interactions in which she is currently involved. Figure 4 shows the online recognition process performed by the Social Context module. Consider, for example, that in a given time window t the local user is having a face-to-face interaction with two colleagues (b and c), while she also receives a message from an old friend (a) she hasn’t heard for a long time. Such information is firstly extracted from the raw sensors data; then, based on the social weights calculated by using Equation 3, b and c are placed in the 2nd and 3rd layers of the network, respectively. Instead, a is located in the outermost ring, due to her limited amount of interactions with the local user. Finally, our solution classifies the relevance of the current active alters for the local user based on the layers in which they are placed in the ego network, thus producing as output the array SC_t , which clearly indicates that the ego is interacting with three different people located in the 2nd, 3rd, and 4th circles, respectively.

Even though our solution does not assign a semantic label to the active alters (e.g., *relative*, *colleague*, or *friend*), the information contained in the output array is sufficient to model the user’s social context in the mobile environment. Such information can be directly used by both the local device and third-party applications to adapt their functionalities according to user’s social context changes, or it can also be combined with other contextual features to recognize higher-level information, such as the user’s behavior, her preferences, or the general situation in which she is currently involved.

3.2. The Familiar Places module

Among the available context information, location is one of the most common features proposed in the literature to characterize the user’s context in the mobile environment [20, 21]. However, geographical coordinates (i.e., latitude and longitude) simply represent a point in the space, which does not contribute

to the recognition of the user’s situation. In the literature, this drawback has been typically addressed by associating a semantic label with GPS data, thus describing the corresponding most likely point of interest (e.g., *restaurant*, *park*, or *bar*) [66, 67]. However, also this approach presents several shortcomings. Firstly, the selection of the most likely point of interest can be inaccurate due to the GPS approximation error, but also because it does not take into account the unique characteristics of the local user, including her preferences and past behavior. Moreover, it strongly relies on external services to select the most suitable label for a given location, potentially exposing the user to privacy leakages. On the contrary, we propose a valid alternative to characterize the user’s location by keeping both the user’s data and the computation on her local device, exploiting the ego network model to dynamically identify the most relevant locations for the user based on her visit frequencies, without the need of semantic labels collected from external services.

The user’s location can be characterized not only by using GPS coordinates, but also taking into account other sensors data that describe the nearby environment, such as the list of Wi-Fi Access Points (APs) and other wireless-enabled devices in proximity. For example, smart TVs and personal home assistants are common in domestic environments, while the presence of wireless printers in the nearby could indicate that the user is located in a workplace. The Familiar Places module relies on such information and on the layered structure of ego networks to model the familiarity degree of the venue in which the user is currently located. A familiar place can be defined as a geographical area or surrounding environment where the local user spends a relatively long time period of her daily life, with a certain frequency. To this aim, we propose the *ego network of locations* model that automatically recognize the familiarity level of the user’s locations based on both geographical and proximity data.

Figure 5a shows the high-level architecture of the Familiar Places module. It is composed by two main elements: the *Proximity based* and *GPS based* modules, each of them creating an ego network specialized on specific context information. While both the modules rely on Algorithm 1 to incrementally update their ego networks as soon as new context data is available, they mainly differ on the type of data used to represent the alters. The former model infers the familiarity degree of a location based on the presence of familiar devices in proximity. In this case, the alters distributed among the ego network’s circles represent the devices discovered through the use of both BT and WFD scans, and the ego-alter links are weighted according to their contact frequencies with the local device. In other words, the more often a device is discovered in proximity of the user, and the more familiar the corresponding location will be. However, as we pointed out in the previous section, wireless scan results can be noisy, including devices that are not relevant for inferring the user’s location. To this aim, similarly to the filtering procedure performed by the Social Context module, we take into account only the context information related to smart objects in proximity, including printers, smart bulbs, and smart TVs, based on the information collected by using the WFD and BT communication protocols. Therefore, we define the strength of the link between the ego and an alter a ,

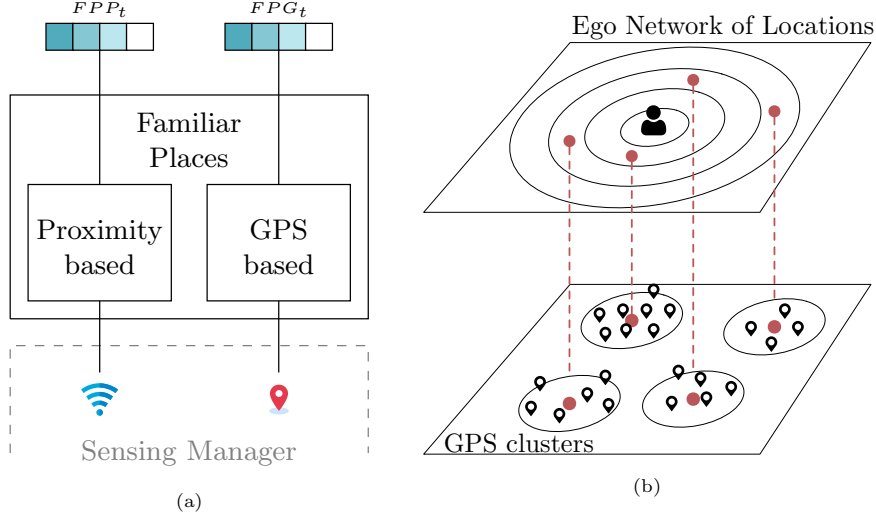


Figure 5: Proposed solution to characterize the user’s location. Figure (a) shows the high-level schema of the functionalities provided by the Familiar Places module, while Figure (b) shows the mapping between GPS clusters and the alters modelled by the user’s ego network.

$\omega_l(a)$, as the total time the two devices have been in proximity of each other, multiplied by the number of their contacts. Formally, we define $\omega_l(a)$ as follows:

$$\omega_l(a) = \begin{cases} (n_a + 1) \cdot \Delta_{a_{t-1}, a_t} & \text{if } \Delta_{a_{t-1}, a_t} \leq \delta \\ n_a + 1 & \text{else} \end{cases}, \quad (4)$$

where n_a is the number of times the device a has been discovered in proximity of the local user, Δ_{t_1, t_2} represents the difference between two timestamps, and δ is the maximum time to consider two different observations as part of the same contact window. This formulation allows the system to keep in memory only a small amount of information for each alter (i.e., $\omega_l(a)$, n_a , and a_t), and to update its associated weight as soon as new data is collected from the sensors available on the mobile device. Finally, the ego-alter weights calculated with Equation 4 are then clustered by Algorithm 1 to define the hierarchical structure of the ego network, and consequentially classify the user’s location based on its familiarity degree.

On the other hand, the *GPS based* module implements a different approach, inferring the user’s familiar places by processing GPS data. Similarly to the previous model, we use the ego network to discriminate between familiar and occasional venues visited by the user. However, due to GPS approximation errors, geographical data can be particularly noisy, and different coordinates can actually represent the same place. To cope with this issue, we firstly cluster raw GPS data to identify the actual location visited by the user, and then we build the ego network of locations by using the clusters centers as alters (as shown in Figure 5b).

It is worth noting that, theoretically, GPS clusters can be identified by using every density-based clustering algorithm, such as the well known DBSCAN [68]. However, traditional (i.e., offline) clustering requires to keep all the data samples in memory and to process them several times to find the best clusters' configuration that optimizes a given metric (e.g., the average squared Euclidean distance in K-means), which is not feasible for memory-constrained devices like smartphones and wearables. Therefore, to preprocess the GPS data on the local device, the GPS based module relies on COMPASS, an online clustering algorithm we recently proposed in the literature to identify hidden patterns from mobile sensors data streams [24]. The algorithm has been compared with the state-of-the-art, both for offline and online clustering approaches, demonstrating to outperform the reference algorithms. Specifically, it uses each observation only once to update its model, and keeps in memory only the necessary information to describe each cluster (i.e., center, radius, and density), instead of processing all the data samples several times to identify the clusters' configuration.

In this case, the cluster's density is calculated by using Equation 4, thus representing both the number of times the local user has visited the venue represented by the identified cluster and the total amount of time she spent in that location. Then, the clusters' centers are considered as alters and further processed by Algorithm 1 to extract the layered structure of the GPS-based ego network, thus automatically discriminating between familiar and occasional venues.

At a given time t , the final output of the Familiar Places module is represented by two distinct arrays, FPP_t and FPG_t , representing the familiarity level of the current user's location with respect to the list of devices in proximity and GPS coordinates, respectively. Third-party applications, as well as other middleware components, can easily request to the Familiar Places module which output array they prefer to use to characterize the user's location, even selecting both of them to model the user's context by taking into account a broader set of features.

4. Experimental evaluation

In this section, we perform two different types of experiments to evaluate the effectiveness of the proposed Social Context and Familiar Places modules to correctly describe the user's social context and location in terms of extracted features from mobile sensors data. As a first step, we assess the structure of both social and location ego networks by using 5 real-world datasets collected from commercial smartphones. Specifically, we identify the exact number of layers required to model the user's social relationships and familiar places in the mobile scenario, by analyzing in detail how the alters (i.e., both people and locations) are distributed among those layers and comparing our findings with the reference literature.

Then, we differentiate our proposal from the related works by providing a semantic evaluation of the models. In fact, previous works typically validate only

the structural characteristics of the ego networks (i.e., their topology) because they extract the social interactions from big data, where the Ground Truth relationships among the users are unknown (e.g., data crawled from OSN). On the contrary, we use smaller datasets, but containing the true nature of the social relationships and the relevance of the visited locations for the local user. This allows us to validate the distribution of the alters among the ego network’s layers from a semantic point of view, assessing, for example, that the most important social relationships of the user and her most familiar places are correctly located within the first layers of the ego network, while the model gives less importance to weak social ties and occasionally visited venues, placing them in the outermost layers of the network.

4.1. Datasets

In order to perform reproducible experiments, we use the following real-world and publicly available datasets that have been collected from personal mobile devices, including both smartphones and smartwatches:

Friends & Family (FF) : this dataset is part of the *Reality Commons* project⁶ and it has been collected in 2011 by the MIT Human Dynamics research group to investigate how people social behaviors affect different aspects of their life, including financial status, physical activity and daily-life decisions [69]. The researchers deployed a sensing application on the personal smartphones of 130 volunteers for over a year, and the resulting dataset includes continuous collection of over 25 phone-based signals, including location, Bluetooth-based device proximity, communication activities (i.e., phone calls and messages), and running applications.

Copenhagen Networks Study (CNS) : contains social data collected from the personal mobile devices of 700 university students over a period of four weeks in 2019 and it is accessible from the figshare repository⁷. Specifically, it includes information related to Bluetooth-based proximity, phone calls, text messages, and Facebook friendships among the participants. The main purpose of collecting such information was to study different characteristics of human social systems, such as modeling temporal social networks, investigating the spreading of information on social networks, analyzing and modeling human mobility, and understanding the interplay between mobility and social behavior [70].

ExtraSensory (ES) : is composed by multi-dimensional sensors data generated by the smartphones of 60 subjects. ES dataset has been collected in 2015-2016 to validate context recognition algorithms in-the-wild, and promoting practical applications that work in real-life mobile settings [71].

⁶<http://realitycommons.media.mit.edu>

⁷<https://doi.org/10.6084/m9.figshare.7267433.v1>

The dataset is freely available on the reference website ⁸, and it contains a total of 300 minutes of measurements, where each data sample is composed by 228 features extracted from both physical and virtual sensors, including accelerometer, gyroscope, user location, and phone conditions (e.g., app status, battery level, and Wi-Fi availability).

MyDigitalFootprint (MDF) : similarly to ES, MDF dataset has been collected in 2018 to model and recognize the user’s context in mobile environments [72]. It is available on Github ⁹, and it includes two months of measurements and information collected by the personal mobile devices of 31 volunteer users, in their natural environment, without limiting their usual behavior. Specifically, 25 volunteers were high-school students of three different cities, while 7 were researchers and Ph.D. students working in the same research center. Compared to ES, MDF contains also relevant information that can be used to characterize the users’ social context and preferences, including Wi-Fi Direct and Bluetooth proximity data, along with information related to the users’ activity on Facebook.

UbiqLog (UL) : this dataset has been collected in order to characterize daily-life events by using smartphone-embedded sensors [73, 74], and it is available on the public UCI Machine Learning repository ¹⁰. The data collection has been conducted in 2013 with 35 participants, for a period of one month. During this period, a mobile application installed on the volunteers’ devices monitored different sensors and events, including running applications, text messages, user’s location, physical sensors (e.g., accelerometer and compass), Bluetooth devices and Wi-Fi Access Points in proximity.

4.2. Social Context evaluation

The first step in building the user’s ego network is to set the number of circles in which the alters will be distributed. This parameter usually depends on the type of social interactions considered to model the social ties among the ego and the alters. While social networks in the physical world are commonly characterized by four layers [75], five circles are a common finding for OSN [76]. Since our objective is to model all the aspects of the users’ social context in the mobile environment by taking into account social interactions in both physical and cyber worlds, we firstly need to find the optimal number of circles to use in our model.

To this aim, we combine the different social signals available in the FF, CNS, and MDF datasets in one single dataset. Specifically, we take into account the data logs related to Bluetooth and Wi-Fi Direct scans, phone calls, and text messaging. In addition, to characterize the users’ social relationships on OSN,

⁸<http://extrasensory.ucsd.edu>

⁹<https://github.com/contextkit/MyDigitalFootprint>

¹⁰[https://archive.ics.uci.edu/ml/datasets/UbiqLog+\(smartphone+lifelogging\)](https://archive.ics.uci.edu/ml/datasets/UbiqLog+(smartphone+lifelogging))

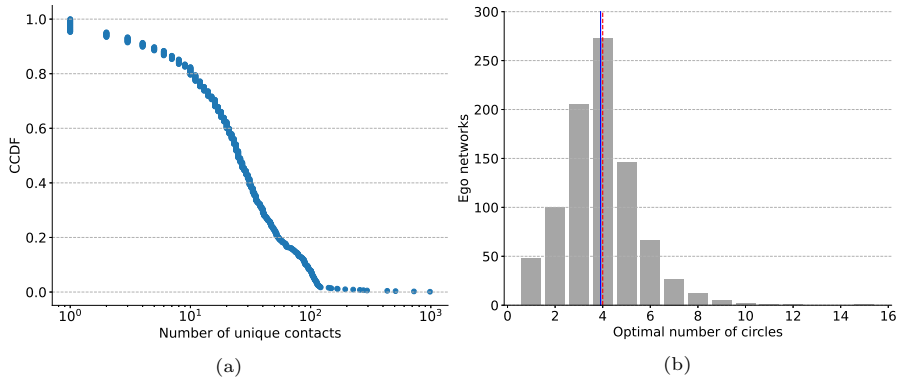


Figure 6: Distribution of the social interactions contained in the FF, CNS, and MDF datasets (a), and the optimal number of circles for the social ego networks (b). Mean and median values are represented by the blue-continuous and red-dashed lines, respectively.

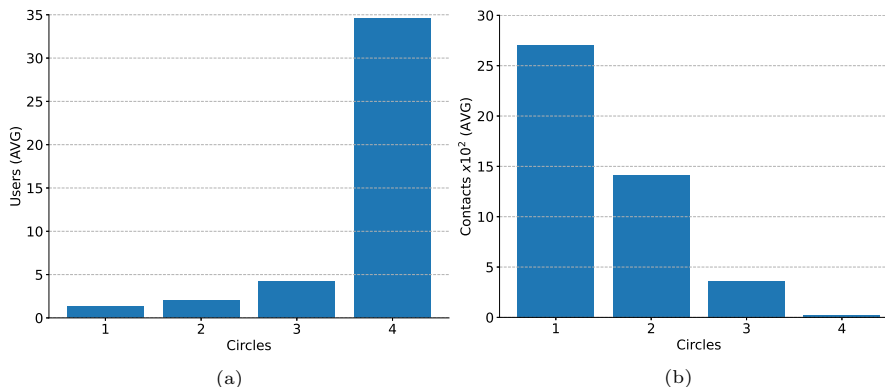


Figure 7: Average number of users located in the different circles of the ego networks (a), and their related contact frequencies with the egos used to weight their social relationships (b).

we also include the Facebook activities contained in the MDF dataset, including comments, reactions and people mentioned (i.e., tagged) in their shared contents (i.e., posts, videos, and photos). The final dataset is composed by 6,993,147 social interactions among 887 users. Please note that each user is analyzed by using her own data, and we combine the aforementioned datasets only to the purpose of obtaining a reliable estimation of the optimal number of circles in our reference scenario.

Figure 6a shows the Complementary Cumulative Function (CCDF) of the unique number of people with whom each user had social interactions. As we can note, it is a long-tailed distribution, where 80% of the users had social interactions with at least 10 people, while only 10% interacted with more than 100 users.

According to the literature [48], we find the optimal number of circles through cluster analysis by using the non-parametric clustering algorithm Meanshift [77].

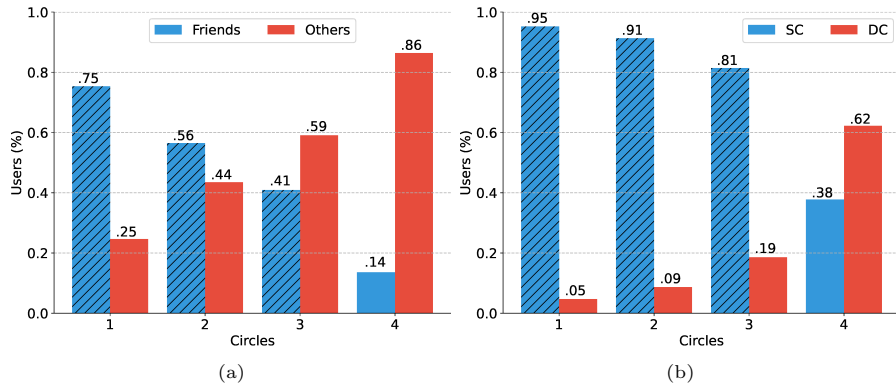


Figure 8: Semantic evaluation of the Social Context module by using the CNS (a) and MDF (b) datasets. The most relevant social relationships (i.e., **F**riends in CNS and people belonging to the same community - **SC** - in MDF) are located within the most inner circles of the ego networks, while people who have occasional social interactions with the egos (i.e., **O**thers in SNC and members of other communities - **DC** - in MDF) are predominant within the outermost circles.

The ego network’s links are weighted by using Equation 3, and we set $\gamma = 0.5$ to equally consider both the user’s virtual and physical social interactions with other people. Figure 6b shows the optimal number of circles found by Meanshift for each user in our dataset, where the continuous-blue and dashed-red lines represent the mean and median values, respectively. As we can note, on average, the best number of layers required to model the user’s social relationships in our reference scenario is 4, which is in accordance with the results found in the literature individually for physical and cyber social interactions data. Figure 7 shows the inner characteristics of the ego networks extracted from the dataset by using the optimal number of circles. Specifically, Figure 7a shows the average number of alters contained in each circle, while Figure 7b presents the average number of contacts (i.e., social interactions) between the ego and the alters. It is worth noting that the most inner circles host only a few people but with a very high contact frequency with the ego, possibly representing her stronger social relationships among those modeled by the ego network. On the contrary, the outermost circles contain a considerable high number of people with whom the ego has few contacts, thus representing occasional social interactions.

In order to further validate the effectiveness of our approach, we analyze the obtained ego networks from a semantic point of view. Specifically, we investigate the nature of the social relationships between the ego and the alters, based on the circles in which they are located. To this aim, we use those datasets where the Ground Truth is available, that is CNS and MDF. In the former dataset we know whether two users are also friends on Facebook, while in MDF the community of each single user is available (i.e., the school class and workplace).

Figures 8 shows the average percentage of users located in each circle, based on the nature of the relationships between the alters and the egos. Specifi-

cally, Figure 8a shows the percentage of Facebook friends and non-friends users (referred to as **Others**) located in each layer of the ego networks.

As we can note, the ego network approach correctly ranks the users’ social interactions according to their strength, distributing the majority of the friends within the first circles. On the other hand, less important relationships represent only a small percentage of the total interactions considered in the first layers, while they are predominant in the outermost circles. This is even more evident in the results obtained by using the MDF dataset shown in Figure 8b. In this case, more than 80% of the alters located in each of the first three layers represent people belonging to the same social community of the ego (**SC**, e.g., colleagues and school mates), while less importance is given to interactions related to people belonging to different communities (**DC**), which represent the majority only in the last circle.

The obtained results clearly show the effectiveness of our approach in modeling the user’s social context by taking into account different types of information characterizing social interactions with other people. In fact, according to the results shown in Figure 8, if a person is classified as a member of the first circles, she probably represents a close friend or a colleague of the local user. On the other hand, if the user’s context is characterized by the presence of alters classified within the outermost circles, the system can surely infer that she is interacting with people occasionally met during her daily life or, however, people not belonging to her closest social relationships.

4.3. Familiar Places evaluation

To evaluate the effectiveness of the Familiar Places module, we firstly extract two distinct sets of data from the datasets presented in Section 4.1. The first set is composed by observations related to those devices in proximity that can characterize the user’s location, such as Wi-Fi APs, smart TVs, printers, and home personal assistants. We refer to this set as proximity-based dataset. Specifically, it includes 4,277,823 data samples related to 204 users contained in the FF, MDF, and UL datasets. Instead, the latter set is composed by GPS traces available in the UL, MDF, and ES datasets, for a total of 1,093,158 observations obtained from 117 users. We refer to this set as GPS-based dataset.

Figure 9 shows the main peculiarities of these two datasets considered for Familiar Places evaluation. Specifically, Figure 9a shows the distribution of the number of unique devices in proximity in the proximity-based dataset, while Figure 9b presents the distribution of unique GPS locations visited by the users in the GPS-based dataset. These datasets contain far more observations compared to the ones used in Section 4.2 for user’s social context modeling. In fact, as we can note, 60% of the users contained in the proximity-based dataset has been in contact with more than 100 devices, while in the GPS-based one, the same percentage of users is associated with at least 1000 unique GPS locations. This is mainly due to the following reasons. Firstly, wireless technology is nowadays embedded in several devices and objects, allowing our personal mobile devices to potentially discover (and being in contact with) even hundreds of devices every day. Secondly, GPS data can be extremely noisy, especially in indoor

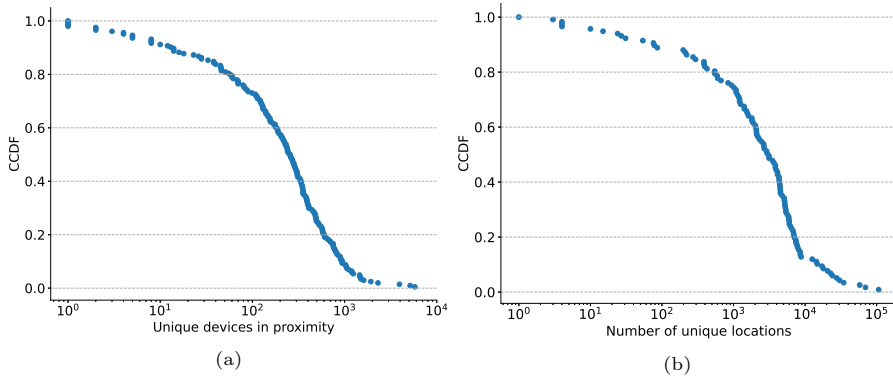


Figure 9: Characteristics of the datasets used to evaluate the ego networks of locations. Figure (a) shows the distribution of the number of unique devices in proximity, while Figure (b) shows the distribution of the unique locations visited by the users based on GPS traces.

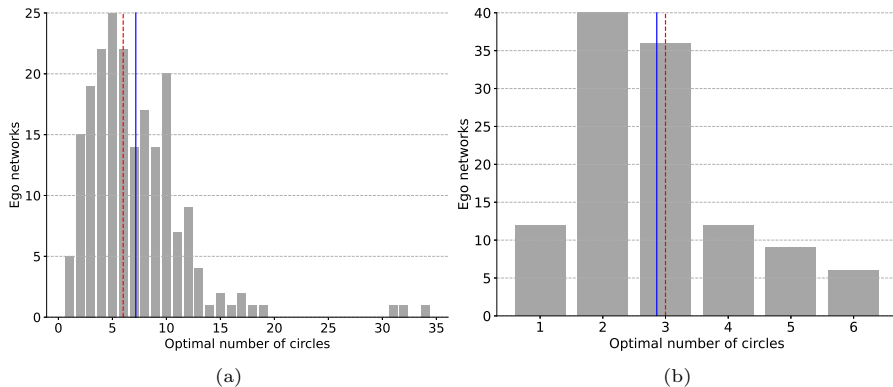


Figure 10: Optimal number of circles for the ego networks of locations based on proximity (a) and GPS data (b). Mean and median values are represented by the blue-continuous and red-dashed lines, respectively.

locations, and several observations can actually refer to the same geographic location. To deal with this issue, the Familiar Places module pre-processes the raw GPS data by using COMPASS online clustering algorithm to identify the actual places visited by the local user. In this way, the 4 millions observations contained in the GPS-based dataset are finally reduced to 1,196 locations and, on average, each user is associated with only 10 clusters.

Since all the necessary information have been extracted from the original datasets, we can now define the structure of the two types of ego networks of locations by following the same approach used to model the user’s social context. Firstly, we calculate the weight of the ego-alter links by using Equation 4 and setting $\delta = 5$ minutes, which defines the maximum interval time between two consecutive observations to update the total time spent by the user in their reference location. Then, we use the Meanshift algorithm to find the optimal

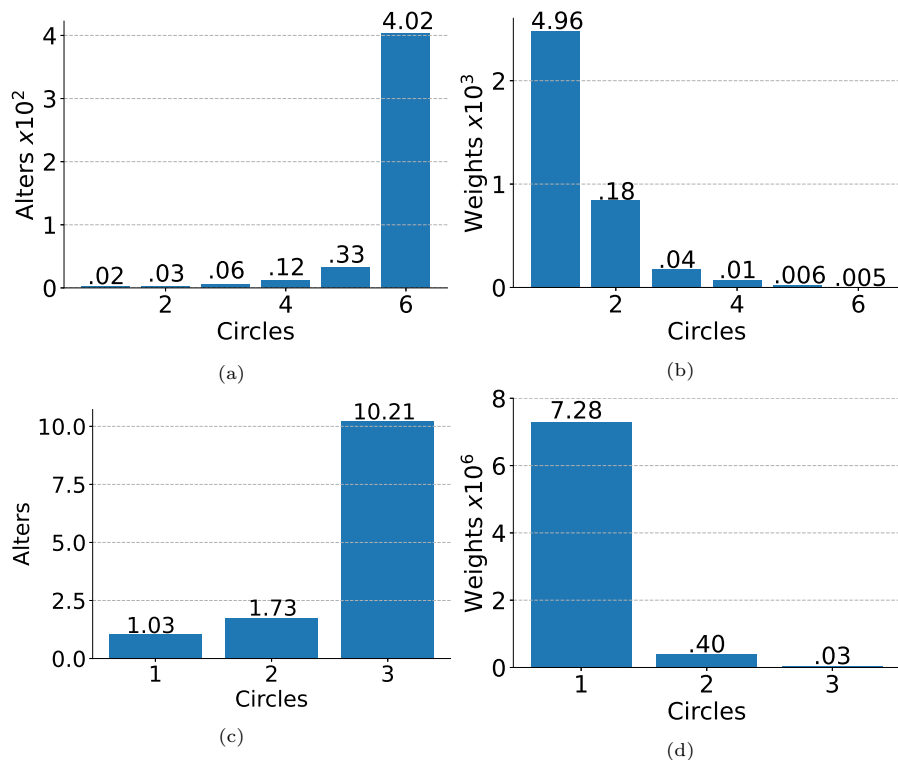


Figure 11: Ego networks of locations structure details. Specifically, Figures (a) and (b) show the average number of alters located in the different circles of the proximity-based model and the value of their associated weights, respectively. The same characteristics are presented for the GPS-based ego networks in Figures (c) and (d).

number of circles of the two types of ego networks by clustering the alters according to their associated weights. Figures 10a and 10b show the optimal number of circles for the proximity-based and GPS-based ego networks of locations, respectively. As we can note, both the distributions considerably differ from the one we obtained with social data, mainly due to the cardinality and nature of the datasets: while the number of circles of the proximity-based ego networks are in the range $[1, 34]$, the ones obtained for the GPS-based model are rather less, arranged between 1 and 6. Despite the difference, the optimal numbers of circles found for the ego networks of locations (i.e., 6 for the proximity-based and 3 for the GPS-based) are comparable to the one proposed in the literature for social interactions' modeling, allowing us to keep the structure of the ego networks simple, and thus, model only the most relevant places visited by the users.

The detailed characteristics of the obtained ego networks of locations are shown in Figure 11. As we expected, in both models, the alters are correctly distributed among the available circles, according with their associated weights.

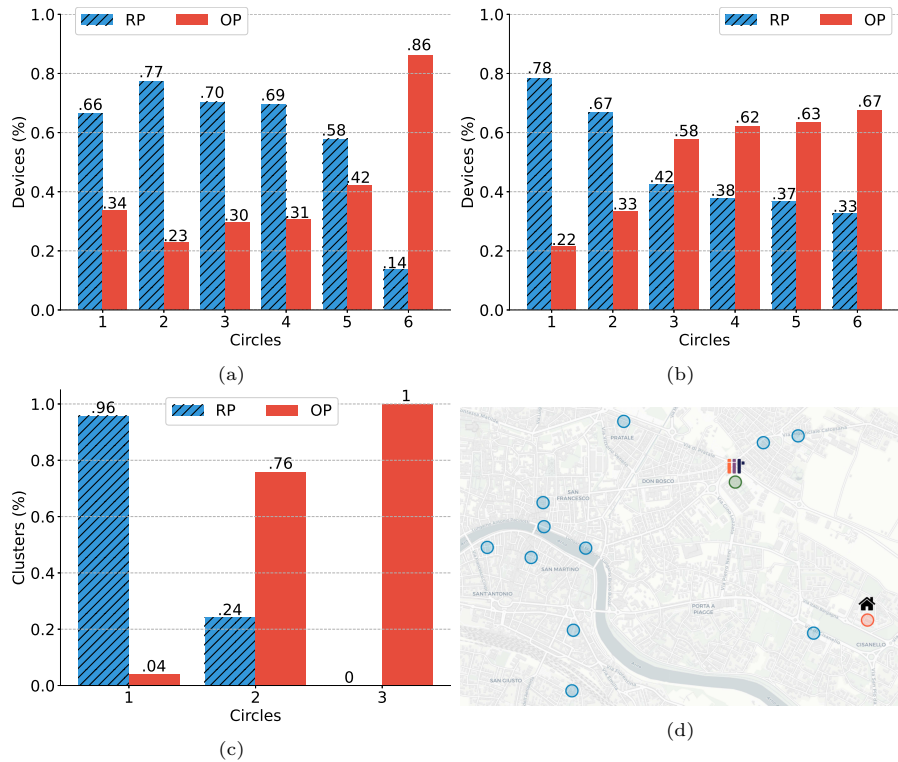


Figure 12: Semantics evaluation of the ego networks of locations. The figures show the locations of both relevant (RP) and occasional (OP) places within the ego networks’ circles. Specifically, Figures (a) and (b) respectively show the results for the proximity-based ego networks by using the MDF and FF datasets, while Figure (c) shows the results obtained from the GPS-based model based on MDF. Figure (d) shows the geographical representation of the GPS clusters classified by the GPS-based model. The clusters are colored based on their associated layer in the ego network: red for the first circle, green is the second, and blue is the third.

The proximity-based model (Figures 11a and 11b) puts the most familiar locations within the first layers, and they are characterized by only a few devices (on average, only 2 and 3 devices in the first two circles, respectively), but with an extremely high contact frequency (i.e., the average weight value associated with the devices in the first layer is almost 5×10^3). Similarly, the most frequently visited GPS clusters (Figures 11c and 11d) are located in the first 2 layers, while the rest, which is the majority, represents occasional places, rarely visited by the user and just for a short time.

We now evaluate the effectiveness of the proposed ego networks to identify the most familiar places among the location visited by the users with respect to the Ground Truth contained in both MDF and FF. Specifically, in the proximity-based dataset both the proximity and GPS data are associated with labels describing the daily life situation in which the user was involved when

she was visiting those places, while in the GPS-based dataset only the list of Wi-Fi APs in the nearby of the user is available. Here, we refer as **Familiar Places (FP)** the set of sensors data associated with labels that describe common relevant locations (e.g., *Home*, *Workplace*, *School*), while **Occasional Places (OP)** represent labelled data that characterizes other situations (e.g., *Free Time*, and *Holiday*).

Figures 12a and 12b show the results obtained by the proximity-based ego networks of locations by using the sets of data extracted from MDF and FF, respectively. Moreover, Figure 12c shows the percentage of FP and OP in each circle of the GPS-based models extracted from MDF. It is worth noting that the percentage of FP is predominant in the most inner circles of both models, correctly highlighting the most relevant locations visited by the users. On the other hand, the presence of OP increases as we observe the data located in the outermost layers of the ego network, representing the great majority of the observations placed in the last circle.

To further demonstrate the effectiveness of the Familiar Places module, we analyze the classification results obtained from the GPS data of a researcher contained in the MDF dataset. Figure 10b shows the geographical clusters extracted by COMPASS from the GPS trace of the user, where each cluster is colored according to the ego network’s circle in which it is located: red for the first circle, green represents the second circle, and blue is used to illustrate the clusters that belong to the outermost layer. Moreover, the figure highlights the two clusters representing the user’s home location and workplace (indicated with IIT), respectively. The obtained result clearly shows the capability of the proposed approach to correctly identify the most familiar places visited by the users, placing both her workplace and home locations within the first two circles. On the other hand, the clusters that represent venues sporadically visited by the user, such as restaurants, gyms and supermarkets, are properly placed in the last circle and, therefore, classified as OP.

5. Complexity evaluation

The main purpose of our work is to define a lightweight solution to characterize the user’s social context and her familiar places as fast as possible by relying on the computational resources available on modern mobile devices. Both the Social Context and Familiar Places modules are based on Algorithm 1, which incrementally updates the ego network model online, as soon as new context data is available from the underlying sensors.

As part of its input, the algorithm requires $\mathcal{W} = [w_{a1}, w_{a2}, \dots, w_{an}]$, the list of weights calculated for the current active alters that must be evaluated to possibly update the current ego network model. Its computation requires negligible time to update the alters’ weights based on the information extracted from the context data sources. According with Equation 3, for the Social Context module, an alter’s weight, ω_a , simply represents the number of times in which the alter appears in the virtual (S_v) and physical (S_p) social data sources, thus requiring $\mathcal{O}(S_v + S_p)$ time to perform such a computation.

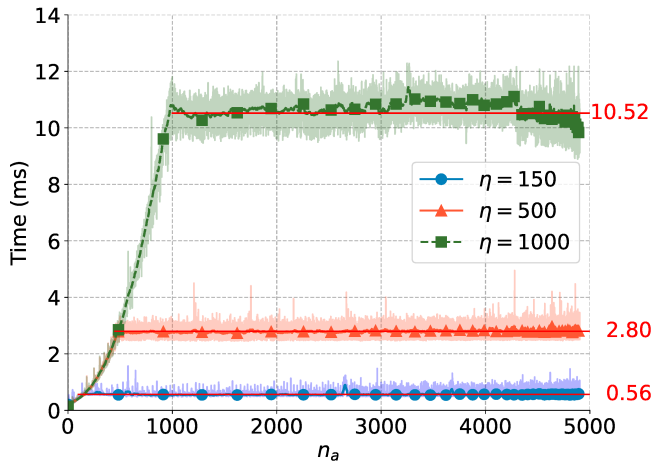


Figure 13: Time required to update the ego network model with an increasing number of unique alters encountered by the ego (n_a) and 3 different values of η , the maximum number of alters to include in the model. The red and continuous lines show the average times to update the model when the ego network reaches the η value.

On the other hand, the execution time required to calculate ω_a in the Familiar Places module mainly depends on the type of context data to process. While for proximity data Equation 4 has a constant time complexity $\mathcal{O}(1)$ because it simply incrementally updates the total time an alter has been in proximity of the local device, GPS data processing requires a pre-clustering phase, which can be efficiently performed in just a few milliseconds with an online clustering algorithm like COMPASS [24].

Both for the Social Context and Familiar Places modules, once ω_a has been calculated, Algorithm 1 performs two main steps: it updates the alters ranking and, if necessary, the ego network model. While the former operation can be performed in $\mathcal{O}(n)$ (e.g., by using a linked list data structure), the latter represents the most time consuming part of the whole algorithm. Actually, in order to distribute the alters among the ego network layers based on their associated weights, a Hierarchical Clustering (HC) [62] algorithm is required. This type of algorithms typically have a time complexity of $\mathcal{O}(n^3)$ (where n is the number of elements that must be clustered), but better performances can be obtained by using efficient agglomerative clustering methods that have a complexity of $\mathcal{O}(n^2)$, such as SLINK [78].

Even though $\mathcal{O}(n^2)$ is not optimal, Algorithm 1 further limits this time complexity by introducing η , an upper-bound of the number of alters that must be taken into account by a given ego network. As we discussed in Section 3.1, $\eta = 150$ is broadly used to model the most relevant social relationships of an individual, while 500 and 15 are the upper-bounds we empirically found in Section 4.3 to successfully characterize the user’s locations based on both proximity and GPS data, respectively.

In order to assess the performances of Algorithm 1 to be executed on resource-

constrained devices and to update the ego network model in real-time, we perform a set of experiments to evaluate the execution time of HC by setting 3 different values of η : 150, 500, and 1000 alters. Specifically, we created a synthetic dataset composed by 20,000 randomly generated contacts between the ego and a population of 5,000 alters, which can represent either other devices in proximity or GPS locations visited by the user. Even though our algorithm updates the ego network only when the first η positions in the alters’ ranking change, in this experiment we execute HC at each contact, thus simulating the worst-case scenario in which the user’s context continuously changes.

Figure 13 shows the time required to update the ego network in the 3 considered settings. Such measurements have been performed on a common laptop (i.e., a MacBook Pro with Intel i7-9750H 6-core a 2,6 GHz processor) by forcing a single-core computation to simulate the execution on a resource-constrained devices. It is worth noting that the execution time rapidly increases according to the number of encountered alters (n_a), but it stabilizes once n_a reaches the upper-bound η . Specifically, the average execution time to update the ego network model is 0.56 ms with $\eta = 150$, 2.80 ms with $\eta = 500$, and 10.52 ms for $\eta = 1000$. The obtained results clearly show that the proposed approach can be entirely executed on the mobile device by processing sensors data in a few milliseconds, thus providing to both the user’s device and third-party applications the ability to quickly adapt and, consequently, react to the changes in the user’s context in a mobile setting.

6. Proof-of-concept application: using the extracted features to recognize daily life situations

The output produced by the proposed modules can be used either to adapt the status and behavior of the mobile device and applications, or as semantic-rich features to automatically recognize the user’s context. In this section, we assess the ability of the features extracted by the Social Context and Familiar Places modules to improve the recognition of daily life situations by using a broad set of smartphone-embedded sensors data and state-of-the-art machine learning algorithms.

For this set of experiments, we use the MDF dataset, which is the most comprehensive one. It is composed by 67,216 data samples, where each of them characterizes a 1-minute snapshot of the user’s context. Specifically, each data sample is represented by a high-dimensional vector of 57 features extracted from the following set of heterogeneous smartphone sensors and data sources: *user gait*, *audio state*, *charging state*, *display status*, *weather conditions*, and *Wi-Fi connection status*. Since the available data describes both the user’s physical activity and her device status, we refer to this set of information as the user’s **Physical Context (PC)**. Moreover, the data samples are associated with labels describing different daily life situations, including *Free time*, *Holiday*, *Home*, *School*, and *Working*. Figure 14 shows the number of samples available for each label. The dataset is highly imbalanced; the great majority of the

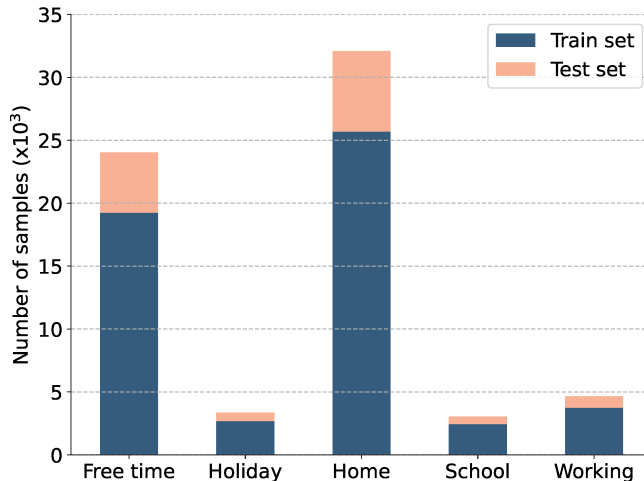


Figure 14: Train and test sets extracted from MDF for the context recognition task.

data belongs to the *Holiday* and *Home* classes, while the others are distributed among *Working*, *School*, and *Holiday*.

To evaluate the semantic expressiveness of the features extracted by the Social Context and Familiar Places modules, we combine them with PC, thus creating 4 different features sets: (i) a baseline set, containing only the physical context information, (ii) PC+SC, which combines the physical and social contexts, (iii) PC+FP, which takes into account both the physical context and the features extracted by the Familiar Places module, and (i) All, which includes all the available features. We then use these features sets to compare the performances of three different types of machine learning classifiers typically used in the literature for user’s activity recognition based on mobile sensors data [79]: Decision Tree (DT), Random Forest (RF), and Deep Neural Network (DNN). DT is a tree-based prediction model, where leaves represent the target classes, while branches represent conjunctions of input features that lead to those class labels. The main goal of DT is to automatically learn the branch splits that best fit the input data. RF is an ensemble of a number of DT trained on various sub-samples of the original dataset to increase the prediction power of the whole model. The final output of RF is obtained by averaging the results produced by the trained DTs.

DNN learns a non-linear function $f(x; \theta) = \hat{y}$, where x is the input vector, \hat{y} represents the predicted label, and θ is the set of model’s parameters learned by using a gradient descent optimization algorithm. To define the DNN architecture we follow the traditional approach for multi-class classification. Specifically, we use the *Rectified Linear Unit (ReLU)* as activation function for the hidden layers, and the output layer is composed by 5 output units, one for each of the considered context classes, which implement the *Softmax* activation function to ensure the output values are in the range of $[0, 1]$ and may be used as predicted

probabilities. To evaluate the predicted label and then update the model parameters accordingly, we use the well-known *Categorical Cross Entropy* loss function that calculates the discrepancy between the actual and predicted labels when the classification problem includes two or more classes. Then, the model’s parameters are updated by using the Adamax optimization algorithm [80]. Moreover, to speed-up the learning process, we use *Batch normalization* [81] that normalizes and scales the activation output of the hidden layers, and, finally, we rely on the *Dropout* [82] algorithm to randomly deactivate hidden units during the training, thus avoiding the overfitting of the final model.

As shown in Figure 14, the MDF dataset is highly skewed, where some classes appear more frequently than others. Even though this is a common characteristic for real-world datasets, it can negatively influence the generalization and reliability of machine learning algorithms, biasing the classification results towards the majority classes [83]. Therefore, to deal with this issue, we compare the performance of the considered machine learning algorithms in terms of *Area Under the Receiver Operating Characteristics (AUROC)*, which is an effective metric to evaluate classifiers with imbalanced datasets [84, 85]. The AUROC describes the binary classification performance of a model comparing the true positive rate with the false positive rate at various threshold settings. To use it in our multi-class classification problem, we followed the One-vs-Rest approach by computing the AUROC of each class against the rest of the available labels and, then, calculating the average score obtained by each class [86]. The evaluation metric is defined in $[0, 1]$, where 0.5 corresponds to the accuracy of a random guesser (i.e., a model that provides random classification) and 1 represents the perfect match between the provided predictions and the Ground Truth. Moreover, in order to evaluate the algorithms performances in detail, we also consider two additional classification metrics: Precision and Recall. The former evaluates the ability of the classifier not to label as positive a sample that is actually negative, and it can formally be defined as the ratio $\frac{tp}{(tp+fp)}$, where tp is the number of *true positive* and fp represents the number of *false positive* predictions. On the other hand, Recall evaluates the ability of the classifier to correctly identify all the positive samples among a collection, and it is defined as $\frac{tp}{(tp+fn)}$, where fn is the number of *false negative* predictions. Similarly to AUROC, both Precision and Recall can be used for a multiclass classification problem with imbalanced datasets by calculating the metrics for each label, and then finding their average value, weighted by the number of true instances for each label.

To avoid biasing the results to a specific train/test sets split (thus possibly obtaining an optimistically evaluation of the model performance), we perform a *5-fold nested cross-validation*: the entire dataset is firstly divided into 5 non-overlapping folds; then, each fold is used as held back test to validate the performance of the model, while all the other folds are collectively used as training dataset. Moreover, to overcome the problem of overfitting the trained model, an inner 5-fold cross-validation is performed over the training dataset both for model selection and hyperparameter tuning. To this aim, we adopted two dif-

Table 2: Classification results for each features set. The best results for each evaluation metric and feature set are highlighted in boldface.

Algorithm	Features	AUROC	Precision	Recall
DT	PC	0.854	0.663	0.682
	PC+SC	0.797	0.627	0.643
	PC+FP	0.842	0.658	0.691
	All	0.849	0.661	0.692
RF	PC	0.871	0.536	0.630
	PC+SC	0.883	0.590	0.632
	PC+FP	0.900	0.580	0.665
	All	0.906	0.621	0.675
DNN	PC	0.947	0.773	0.777
	PC+SC	0.957	0.804	0.807
	PC+FP	0.957	0.802	0.803
	All	0.965	0.826	0.827

ferent strategies based on the classification algorithm. Specifically, we use the Grid search approach implemented in scikit-learn [87] to perform an exhaustive search over a specified value space for the most important parameters of DT and RF, while we rely on Keras Tuner [88] to find the best DNN configuration by using the Hyperband optimization algorithm [89].

The most important parameters of DT and the corresponding values space we considered are the following: (i) *min sample leaf* ($min_{sl} \in [10, 50, 100, 200]$), the minimum number of training samples used to define a leaf node; and *max depth* ($max_d \in [10, 50, 100, 200]$), that represents the maximum depth of the decision tree. RF shares with DT the first two parameters to define the structure of the decision tree used in the whole model. Additionally, we also tune the parameter *estimators* ($n_e \in [100, 400, 500]$), which defines the number of estimators to use to produce the final prediction. The DNN hyperparameters that we evaluate are the following: *batch-size* ($b_s \in [128, 512, 1024, 200]$), the number of samples that will be propagated through the network at each training step; *dropout-rate* ($d_r \in [0, 0.2, 0.4, 0.6]$), that represents the percentage of neurons that must be deactivated during the model training; *epochs* ($e \in [50, 100, 200, 300]$), the number of training iterations; *hidden layers* ($n_{hl} \in [1, \dots, 5]$), the number of hidden layers; *hidden units* ($n_{hu} \in [100, 200, 300]$), which defines the number of neurons for each hidden layer; and *learning rate* ($l_r \in [0.001, 0.01, 0.1]$), the learning rate value to use with the Adamax optimization algorithm.

Table 2 shows the classification performance of the considered algorithms over the 4 datasets in terms of AUROC, Precision, and Recall. Precisely, we report the average scores over the 5-folds, while we omit their standard deviations because we obtained irrelevant values during the experiments (i.e., less than 0.001). As we can note, the simplest solution, DT, performs worst and it is the only algorithm that does not take advantage of the proposed additional fea-

tures, obtaining its best performance by using only the baseline dataset: 0.854 AUROC, 0.663 Precision, and 0.682 Recall. On the other hand, the ensemble classifier, RF, successfully exploits the combination of our semantic-rich features with the physical context data. Indeed, its classification performances clearly increase when all the features are used, obtaining a gain of approximately 3% in terms of AUROC, 8% of Precision, and 4% of Recall, with respect to the results scored with the PC dataset. Moreover, the use of both SC and FP allows RF to improve the AUROC of DT by 5%, with a slight increase in terms of false positive rate, and a comparable Recall score.

The DNN model clearly overcomes the other two solutions, obtaining, on average, a performance increase of 7% AUROC against RF and 12.75% AUROC with respect to DT, over all the 4 datasets. Specifically, it achieves 0.947 of accuracy with the PC dataset, 0.957 when either the social context or familiar places are included, and 0.965 both our features sets are combined with the physical sensors data. Moreover, the proposed features allows DNN to obtain a gain of 6% in terms of both Precision and Recall, compared with its performance obtained by using only PC. This result is surely due to the ability of the model to learn effective non-linear combination of the input data, but it also proves the great advantage of modeling both the users’ social interactions and her familiar places with the proposed unsupervised approaches.

7. Conclusions and future work

In this paper, we propose two unsupervised algorithms to automatically model the user’s social context and visited location directly on the mobile device based on embedded sensor data. Specifically, we presented the implementation of such algorithms as the *Social Context* and *Familiar Places* modules of a more general middleware solution that support all the tasks required to collect and recognize the user’s context in mobile scenarios. The Social Context module characterizes the user’s social relationships as an ego network, modeling both physical and virtual social interactions based on different signals, including face-to-face contacts inferred by using wireless technologies, phone calls, text messages, and Online Social Networks activities. Based on these data sources, the user’s ego network is extracted by clustering the identified people (alters) based on their contact frequencies with the local user, thus creating a hierarchical structure that classifies the user’s social relationships according to their relevance. Based on a similar approach, the Familiar Places module models the level of familiarity of the user’s locations based on her visiting frequency. Specifically, it creates two distinct ego networks where the alters represent, respectively, GPS locations and smart devices in proximity (e.g., smart TVs and Wi-Fi Access Points).

To evaluate the effectiveness of our proposals, we performed 4 different sets of experiments by using 5 real-world datasets collected by personal mobile devices, including both smartphones and smartwatches. Firstly, we assessed the structure of the proposed ego networks and the distribution of the data among

their layers. Then, we provided a semantic evaluation of the two models, assessing that the most relevant social relationships and familiar places are properly located among the first layers of the model, while the least important are placed on the outermost circles. We determined the theoretical and empirical time complexity of the proposed solutions, proving their effectiveness in quickly adapting the ego network model by performing the entire processing on the local mobile device. Finally, we presented a proof-of-concept application to show the efficacy of the extracted features to recognize the user's context. Specifically, we demonstrated how the performance of 3 different machine learning algorithms improve by using such features to recognize daily-life situations based on smartphone-embedded sensors data.

As part of our future work, we will investigate unsupervised solutions to characterize other aspects of the user's context, including, for example, preferences and habits. Such an information is extremely relevant for service personalization maintaining data and processing on the personal mobile device, at the Edge of the Internet. In addition, we are currently working on the implementation of a prototype of the context-aware middleware including the presented modules. This will allow us to evaluate the algorithms proposed in this paper in real-world scenarios.

Acknowledgement

This work has been partially funded by the European Commission under H2020-INFRAIA-2019-1SoBigData-PlusPlus project. Grant number: 871042.

References

- [1] M. Conti, A. Passarella, The internet of people: A human and data-centric paradigm for the next generation, *Computer Communications* 131 (2018) 51–65, cOMCOM 40 years. doi:<https://doi.org/10.1016/j.comcom.2018.07.034>. URL <https://www.sciencedirect.com/science/article/pii/S0140366418305127>
- [2] M. Satyanarayanan, The emergence of edge computing, *Computer* 50 (1) (2017) 30–39. doi:[10.1109/MC.2017.9](https://doi.org/10.1109/MC.2017.9).
- [3] R. Rawassizadeh, T. J. Pierson, R. Peterson, D. Kotz, Nocloud: Exploring network disconnection through on-device data analysis, *IEEE Pervasive Computing* 17 (1) (2018) 64–74. doi:[10.1109/MPRV.2018.011591063](https://doi.org/10.1109/MPRV.2018.011591063).
- [4] Y. Zhao, W. Song, Survey on social-aware data dissemination over mobile wireless networks, *IEEE Access* 5 (2017) 6049–6059. doi:[10.1109/ACCESS.2017.2693689](https://doi.org/10.1109/ACCESS.2017.2693689).
- [5] P. Hui, J. Crowcroft, E. Yoneki, Bubble rap: Social-based forwarding in delay-tolerant networks, *IEEE Transactions on Mobile Computing* 10 (11) (2011) 1576–1589. doi:[10.1109/TMC.2010.246](https://doi.org/10.1109/TMC.2010.246).

- [6] P. Olla, C. Shimskey, mhealth taxonomy: a literature survey of mobile health applications, *Health and Technology* 4 (4) (2015) 299–308. doi:[10.1007/s12553-014-0093-8](https://doi.org/10.1007/s12553-014-0093-8). URL <https://doi.org/10.1007/s12553-014-0093-8>
- [7] T. S. Buda, M. Khwaja, A. Matic, Outliers in smartphone sensor data reveal outliers in daily happiness, *Proc. ACM Interact. Mob. Wearable Ubiquitous Technol.* 5 (1) (Mar. 2021). doi:[10.1145/3448095](https://doi.org/10.1145/3448095). URL <https://doi.org/10.1145/3448095>
- [8] H. Vahdat-Nejad, A. Ramazani, T. Mohammadi, W. Mansoor, A survey on context-aware vehicular network applications, *Vehicular Communications* 3 (2016) 43–57. doi:<https://doi.org/10.1016/j.vehcom.2016.01.002>. URL <https://www.sciencedirect.com/science/article/pii/S2214209616000036>
- [9] S. Krings, E. Yigitbas, I. Jovanovikj, S. Sauer, G. Engels, Development framework for context-aware augmented reality applications, in: *Companion Proceedings of the 12th ACM SIGCHI Symposium on Engineering Interactive Computing Systems, EICS '20 Companion, Association for Computing Machinery, New York, NY, USA, 2020*. doi:[10.1145/3393672.3398640](https://doi.org/10.1145/3393672.3398640). URL <https://doi.org/10.1145/3393672.3398640>
- [10] V. Arnaboldi, M. G. Campana, F. Delmastro, E. Pagani, A personalized recommender system for pervasive social networks, *Pervasive and Mobile Computing* 36 (2017) 3–24, special Issue on Pervasive Social Computing. doi:<https://doi.org/10.1016/j.pmcj.2016.08.010>. URL <https://www.sciencedirect.com/science/article/pii/S1574119216301365>
- [11] T. Eichinger, F. Beierle, R. Papke, L. Rebscher, H. C. Tran, M. Trzeciak, On gossip-based information dissemination in pervasive recommender systems, in: *Proceedings of the 13th ACM Conference on Recommender Systems, RecSys '19, Association for Computing Machinery, New York, NY, USA, 2019*, p. 442–446. doi:[10.1145/3298689.3347067](https://doi.org/10.1145/3298689.3347067). URL <https://doi.org/10.1145/3298689.3347067>
- [12] J. Morales, D. Akopian, Physical activity recognition by smartphones, a survey, *Biocybernetics and Biomedical Engineering* 37 (3) (2017) 388–400. doi:<https://doi.org/10.1016/j.bbe.2017.04.004>. URL <https://www.sciencedirect.com/science/article/pii/S020852161630314X>
- [13] M. G. Campana, D. Chatzopoulos, F. Delmastro, P. Hui, Lightweight modeling of user context combining physical and virtual sensor data, in: *Proceedings of the 2018 ACM International Joint Conference and 2018 International Symposium on Pervasive and Ubiquitous Computing and Wearable Computers, UbiComp '18, Association for Computing Machinery,*

New York, NY, USA, 2018, p. 1309–1320. doi:10.1145/3267305.3274178.
URL <https://doi.org/10.1145/3267305.3274178>

- [14] W. Shi, S. Dustdar, The promise of edge computing, *Computer* 49 (5) (2016) 78–81. doi:10.1109/MC.2016.145.
- [15] D. Chen, H. Zhao, Data security and privacy protection issues in cloud computing, in: 2012 International Conference on Computer Science and Electronics Engineering, Vol. 1, 2012, pp. 647–651. doi:10.1109/ICCSEE.2012.193.
- [16] M. Chiang, T. Zhang, Fog and iot: An overview of research opportunities, *IEEE Internet of Things Journal* 3 (6) (2016) 854–864. doi:10.1109/JIOT.2016.2584538.
- [17] Z. Ma, J. Ma, Y. Miao, X. Liu, K.-K. R. Choo, R. Yang, X. Wang, Lightweight privacy-preserving medical diagnosis in edge computing, *IEEE Transactions on Services Computing* (2020) 1–1 doi:10.1109/TSC.2020.3004627.
- [18] Y. Liu, C. Yang, L. Jiang, S. Xie, Y. Zhang, Intelligent edge computing for iot-based energy management in smart cities, *IEEE Network* 33 (2) (2019) 111–117. doi:10.1109/MNET.2019.1800254.
- [19] R. Rawassizadeh, M. Tomitsch, M. Nourizadeh, E. Momeni, A. Peery, L. Ulanova, M. Pazzani, Energy-efficient integration of continuous context sensing and prediction into smartwatches, *Sensors* 15 (9) (2015) 22616–22645. doi:10.3390/s150922616.
URL <https://www.mdpi.com/1424-8220/15/9/22616>
- [20] Ö. Yürür, C. H. Liu, Z. Sheng, V. C. M. Leung, W. Moreno, K. K. Leung, Context-awareness for mobile sensing: A survey and future directions, *IEEE Communications Surveys Tutorials* 18 (1) (2016) 68–93.
- [21] A. Capponi, C. Fiandrino, B. Kantarci, L. Foschini, D. Kliazovich, P. Bouvry, A survey on mobile crowdsensing systems: Challenges, solutions, and opportunities, *IEEE Communications Surveys Tutorials* 21 (3) (2019) 2419–2465.
- [22] H. Zhou, H. Wang, N. Wang, D. Li, Y. Cao, X. Li, J. Wu, Exploiting mobile social networks from temporal perspective: A survey, *IEEE Access* 7 (2019) 180818–180834. doi:10.1109/ACCESS.2019.2958951.
- [23] V. Arnaboldi, M. Conti, A. Passarella, R. I. Dunbar, Online social networks and information diffusion: The role of ego networks, *Online Social Networks and Media* 1 (2017) 44–55. doi:<https://doi.org/10.1016/j.osnem.2017.04.001>.
URL <https://www.sciencedirect.com/science/article/pii/S2468696417300150>

- [24] M. G. Campana, F. Delmastro, Compass: Unsupervised and online clustering of complex human activities
Expert Systems with Applications (2021)
115124doi:<https://doi.org/10.1016/j.eswa.2021.115124>.
URL <https://www.sciencedirect.com/science/article/pii/S0957417421005650>
- [25] P. Paul, T. George, An effective approach for human activity recognition on smartphone, in: 2015 IEEE International Conference on Engineering and Technology (ICETECH), 2015, pp. 1–3. doi:10.1109/ICETECH.2015.7275024.
- [26] M. E. ul Haq, M. Awais Azam, Y. Asim, Y. Amin, U. Naeem, A. Khalid, Using smartphone accelerometer for human physical activity and context recognition in-the-wild, *Procedia Computer Science* 177 (2020) 24–31, the 11th International Conference on Emerging Ubiquitous Systems and Pervasive Networks (EUSPN 2020) / The 10th International Conference on Current and Future Trends of Information and Communication Technologies in Healthcare (ICTH 2020) / Affiliated Workshops. doi:<https://doi.org/10.1016/j.procs.2020.10.007>.
URL <https://www.sciencedirect.com/science/article/pii/S1877050920322729>
- [27] T. Zebin, P. J. Scully, N. Peek, A. J. Casson, K. B. Ozanyan, Design and implementation of a convolutional neural network on an edge computing smartphone for human activity recognition, *IEEE Access* 7 (2019) 133509–133520. doi:10.1109/ACCESS.2019.2941836.
- [28] M. Conti, S. K. Das, C. Bisdikian, M. Kumar, L. M. Ni, A. Passarella, G. Roussos, G. Tröster, G. Tsudik, F. Zambonelli, Looking ahead in pervasive computing: Challenges and opportunities in the era of cyber–physical conver
Pervasive and Mobile Computing 8 (1) (2012) 2–21. doi:<https://doi.org/10.1016/j.pmcj.2011.10.001>.
URL <https://www.sciencedirect.com/science/article/pii/S1574119211001271>
- [29] C. Quadri, M. Zignani, S. Gaito, G. P. Rossi, Feature-rich ego-network circles in mobile phone graphs: Tie multiplexity and the role of alters, in: 2018 IEEE/ACM International Conference on Advances in Social Networks Analysis and Mining (ASONAM), 2018, pp. 1280–1285. doi:10.1109/ASONAM.2018.8508560.
- [30] V. Arnaboldi, M. Conti, A. Passarella, R. Dunbar, Dynamics of personal social relationships in online social networks: A study on twitter, in: Proceedings of the First ACM Conference on Online Social Networks, COSN '13, Association for Computing Machinery, New York, NY, USA, 2013, p. 15–26. doi:10.1145/2512938.2512949.
URL <https://doi.org/10.1145/2512938.2512949>
- [31] D. Camps-Mur, A. Garcia-Saavedra, P. Serrano, Device-to-device communications with wi-fi direct: overview and experimentation, *IEEE Wireless Communications* 20 (3) (2013) 96–104. doi:10.1109/MWC.2013.6549288.

- [32] K. T’Jonck, B. Pang, H. Hallez, J. Boydens, Optimizing the bluetooth low energy service discovery process, *Sensors* 21 (11) (2021). doi:10.3390/s21113812.
URL <https://www.mdpi.com/1424-8220/21/11/3812>
- [33] R.-A. Voicu, C. Dobre, L. Bajenaru, R.-I. Ciobanu, Human physical activity recognition using smartphone sensors, *Sensors* 19 (3) (2019). doi:10.3390/s19030458.
URL <https://www.mdpi.com/1424-8220/19/3/458>
- [34] S.-H. Fang, Y.-X. Fei, Z. Xu, Y. Tsao, Learning transportation modes from smartphone sensors based on deep neural network, *IEEE Sensors Journal* 17 (18) (2017) 6111–6118. doi:10.1109/JSEN.2017.2737825.
- [35] M. Gjoreski, V. Janko, G. Slapničar, M. Mlakar, N. Reščič, J. Bizjak, V. Drobnič, M. Marinko, N. Mlakar, M. Luštrek, M. Gams, Classical and deep learning methods for recognizing human activities and modes of transportation with s, *Information Fusion* 62 (2020) 47–62. doi:<https://doi.org/10.1016/j.inffus.2020.04.004>.
URL <https://www.sciencedirect.com/science/article/pii/S1566253520302566>
- [36] Z. Chen, M. Lin, F. Chen, N. D. Lane, G. Cardone, R. Wang, T. Li, Y. Chen, T. Choudhury, A. T. Campbell, Unobtrusive sleep monitoring using smartphones, in: 2013 7th International Conference on Pervasive Computing Technologies for Healthcare and Workshops, 2013, pp. 145–152.
- [37] L. Ciabattini, F. Ferracuti, S. Longhi, L. Pepa, L. Romeo, F. Verdini, Real-time mental stress detection based on smartwatch, in: 2017 IEEE International Conference on Consumer Electronics (ICCE), 2017, pp. 110–111. doi:10.1109/ICCE.2017.7889247.
- [38] R. Rawassizadeh, E. Momeni, C. Dobbins, J. Gharibshah, M. Pazzani, Scalable daily human behavioral pattern mining from multivariate temporal data, *IEEE Transactions on Knowledge and Data Engineering* 28 (11) (2016) 3098–3112. doi:10.1109/TKDE.2016.2592527.
- [39] Y. Vaizman, N. Weibel, G. Lanckriet, Context recognition in-the-wild: Unified model for multi-modal sensors and multi-label classification, *Proc. ACM Interact. Mob. Wearable Ubiquitous Technol.* 1 (4) (Jan. 2018). doi:10.1145/3161192.
URL <https://doi.org/10.1145/3161192>
- [40] S. Shelke, J. Harbour, B. Aksanli, Building an intelligent and efficient smart space to detect human behavior in common areas, in: 2018 International Symposium on Networks, Computers and Communications (ISNCC), 2018, pp. 1–6. doi:10.1109/ISNCC.2018.8530988.
- [41] K. Davis, E. Owusu, V. Bastani, L. Marcenaro, J. Hu, C. Regazzoni, L. Feijs, Activity recognition based on inertial sensors for ambient assisted

- living, in: 2016 19th International Conference on Information Fusion (FUSION), 2016, pp. 371–378.
- [42] X. Zhang, C. T. Butts, Activity correlation spectroscopy: a novel method for inferring social relationships
Social Network Analysis and Mining 7 (1) (2016) 1.
 doi:[10.1007/s13278-016-0419-9](https://doi.org/10.1007/s13278-016-0419-9).
 URL <https://doi.org/10.1007/s13278-016-0419-9>
- [43] S. Tabassum, F. S. F. Pereira, S. Fernandes, J. Gama, Social network analysis: An overview,
WIREs Data Mining and Knowledge Discovery 8 (5) (2018) e1256.
 arXiv:<https://onlinelibrary.wiley.com/doi/pdf/10.1002/widm.1256>,
 doi:<https://doi.org/10.1002/widm.1256>.
 URL <https://onlinelibrary.wiley.com/doi/abs/10.1002/widm.1256>
- [44] V. Arnaboldi, A. Passarella, M. Conti, R. I. Dunbar, Chapter 2 - human social networks, in: V. Arnaboldi, A. Passarella, M. Conti, R. I. Dunbar (Eds.), *Online Social Networks*, Computer Science Reviews and Trends, Elsevier, Boston, 2015, pp. 9–35.
 doi:<https://doi.org/10.1016/B978-0-12-803023-3.00002-3>.
 URL <https://www.sciencedirect.com/science/article/pii/B9780128030233000023>
- [45] S. G. Roberts, R. I. Dunbar, T. V. Pollet, T. Kuppens, Exploring variation in active network size: Constraints and ego characteristics,
Social Networks 31 (2) (2009) 138–146.
 doi:<https://doi.org/10.1016/j.socnet.2008.12.002>.
 URL <https://www.sciencedirect.com/science/article/pii/S0378873309000033>
- [46] S. B. G. Roberts, R. I. M. Dunbar, Managing relationship decay, *Human Nature* 26 (4) (2015) 426–450. doi:[10.1007/s12110-015-9242-7](https://doi.org/10.1007/s12110-015-9242-7).
 URL <https://doi.org/10.1007/s12110-015-9242-7>
- [47] S. Shultz, R. Dunbar, Encephalization is not a universal macroevolutionary phenomenon in mammals but
Proceedings of the National Academy of Sciences 107 (50) (2010) 21582–21586.
 arXiv:<https://www.pnas.org/content/107/50/21582.full.pdf>,
 doi:[10.1073/pnas.1005246107](https://doi.org/10.1073/pnas.1005246107).
 URL <https://www.pnas.org/content/107/50/21582>
- [48] C. Boldrini, M. Toprak, M. Conti, A. Passarella, Twitter and the press: An ego-centred analysis, in: *Companion Proceedings of the The Web Conference 2018, WWW '18*, International World Wide Web Conferences Steering Committee, Republic and Canton of Geneva, CHE, 2018, p. 1471–1478. doi:[10.1145/3184558.3191596](https://doi.org/10.1145/3184558.3191596).
 URL <https://doi.org/10.1145/3184558.3191596>
- [49] W.-X. Zhou, D. Sornette, R. A. Hill, R. I. M. Dunbar, Discrete hierarchical organization of social group sizes,
Proceedings of the Royal Society B: Biological Sciences 272 (1561) (2005) 439–444.

arXiv:<https://royalsocietypublishing.org/doi/pdf/10.1098/rspb.2004.2970>,
doi:10.1098/rspb.2004.2970.
URL <https://royalsocietypublishing.org/doi/abs/10.1098/rspb.2004.2970>

- [50] J. Zheng, L. M. Ni, An unsupervised learning approach to social circles detection in ego bluetooth proximity: Proceedings of the 2013 ACM International Joint Conference on Pervasive and Ubiquitous Computing, UbiComp '13, Association for Computing Machinery, New York, NY, USA, 2013, p. 721–724. doi:10.1145/2493432.2493512. URL <https://doi.org/10.1145/2493432.2493512>
- [51] D. Yu, Y. Li, F. Xu, P. Zhang, V. Kostakos, Smartphone app usage prediction using points of interest, Proc. ACM Interact. Mob. Wearable Ubiquitous Technol. 1 (4) (Jan. 2018). doi:10.1145/3161413. URL <https://doi.org/10.1145/3161413>
- [52] M. A. Cheema, Indoor location-based services: Challenges and opportunities, SIGSPATIAL Special 10 (2) (2018) 10–17. doi:10.1145/3292390.3292394. URL <https://doi.org/10.1145/3292390.3292394>
- [53] T. M. T. Do, D. Gatica-Perez, Where and what: Using smartphones to predict next locations and applications, Pervasive and Mobile Computing 12 (2014) 79–91. doi:<https://doi.org/10.1016/j.pmcj.2013.03.006>. URL <https://www.sciencedirect.com/science/article/pii/S1574119213000576>
- [54] X. Niu, S. Wang, C. Q. Wu, Y. Li, P. Wu, J. Zhu, On a clustering-based mining approach with labeled semantics for significant place discovery, Information Sciences 578 (2021) 37–63. doi:<https://doi.org/10.1016/j.ins.2021.07.050>. URL <https://www.sciencedirect.com/science/article/pii/S0020025521007404>
- [55] A. Sirbu, G. Andrienko, N. Andrienko, C. Boldrini, M. Conti, F. Giannotti, R. Guidotti, S. Bertoli, J. Kim, C. I. Muntean, L. Pappalardo, A. Passarella, D. Pedreschi, L. Pollacci, F. Pratesi, R. Sharma, Human migration: the big data perspective, International Journal of Data Science and Analytics 11 (4) (2021) 341–360. doi:10.1007/s41060-020-00213-5. URL <https://doi.org/10.1007/s41060-020-00213-5>
- [56] B. Bilecen, M. Gamper, M. J. Lubbers, The missing link: Social network analysis in migration and transnationalism, Social Networks 53 (2018) 1–3, the missing link: Social network analysis in migration and transnationalism. doi:<https://doi.org/10.1016/j.socnet.2017.07.001>. URL <https://www.sciencedirect.com/science/article/pii/S0378873317302575>

- [57] S. Pike, M. Lubell, Geography and social networks in transportation mode choice, *Journal of Transport Geography* 57 (2016) 184–193. doi:<https://doi.org/10.1016/j.jtrangeo.2016.10.009>. URL <https://www.sciencedirect.com/science/article/pii/S0966692316306111>
- [58] K. Ollivier, C. Boldrini, A. Passarella, M. Conti, Structural invariants in individuals language use: The “ego network” of words, in: S. Aref, K. Bontcheva, M. Braghieri, F. Dignum, F. Giannotti, F. Grisolia, D. Pedreschi (Eds.), *Social Informatics*, Springer International Publishing, Cham, 2020, pp. 267–282.
- [59] W. Lucia, E. Ferrari, Egocentric: Ego networks for knowledge-based short text classification, in: *Proceedings of the 23rd ACM International Conference on Conference on Information and Knowledge Management, CIKM '14*, Association for Computing Machinery, New York, NY, USA, 2014, p. 1079–1088. doi:10.1145/2661829.2661990. URL <https://doi.org/10.1145/2661829.2661990>
- [60] R. Xiang, J. Neville, M. Rogati, Modeling relationship strength in online social networks, in: *Proceedings of the 19th International Conference on World Wide Web, WWW '10*, Association for Computing Machinery, New York, NY, USA, 2010, p. 981–990. doi:10.1145/1772690.1772790. URL <https://doi.org/10.1145/1772690.1772790>
- [61] S. Liu, Y. Jiang, A. Striegel, Face-to-face proximity estimation using bluetooth on smartphones, *IEEE Transactions on Mobile Computing* 13 (4) (2014) 811–823. doi:10.1109/TMC.2013.44.
- [62] F. Nielsen, *Hierarchical Clustering*, Springer International Publishing, Cham, 2016, pp. 195–211. doi:10.1007/978-3-319-21903-5_8. URL https://doi.org/10.1007/978-3-319-21903-5_8
- [63] R. I. Dunbar, The social brain hypothesis, *Evolutionary Anthropology: Issues, News, and Reviews: Issues, News, and Reviews* 6 (5) (1998) 178–190.
- [64] C. A. Bliss, I. M. Kloumann, K. D. Harris, C. M. Danforth, P. S. Dodds, Twitter reciprocal reply networks exhibit assortativity with respect to happiness, *Journal of Computational Science* 3 (5) (2012) 388–397, *advanced Computing Solutions for Health Care and Medicine*. doi:<https://doi.org/10.1016/j.jocs.2012.05.001>. URL <https://www.sciencedirect.com/science/article/pii/S187775031200049X>
- [65] Q. Wang, J. Gao, T. Zhou, Z. Hu, H. Tian, Critical size of ego communication networks, *EPL (Europhysics Letters)* 114 (5) (2016) 58004. doi:10.1209/0295-5075/114/58004. URL <https://doi.org/10.1209/0295-5075/114/58004>

- [66] G. Qiu, D. Guo, Y. Shen, G. Tang, S. Chen, Mobile semantic-aware trajectory for personalized location privacy preservation, *IEEE Internet of Things Journal* 8 (21) (2021) 16165–16180. doi:10.1109/JIOT.2020.3016466.
- [67] H. Cao, F. Xu, J. Sankaranarayanan, Y. Li, H. Samet, Habit2vec: Trajectory semantic embedding for living pattern recognition in population, *IEEE Transactions on Mobile Computing* 19 (5) (2020) 1096–1108. doi:10.1109/TMC.2019.2902403.
- [68] M. Ester, H.-P. Kriegel, J. Sander, X. Xu, et al., A density-based algorithm for discovering clusters in large spatial databases with noise., in: *Kdd*, Vol. 96, 1996, pp. 226–231.
- [69] N. Aharony, W. Pan, C. Ip, I. Khayal, A. Pentland, Social fmri: Investigating and shaping social mechanisms in the real world, *Pervasive and Mobile Computing* 7 (6) (2011) 643 – 659, the Ninth Annual IEEE International Conference on Pervasive Computing and Communications (PerCom 2011). doi:https://doi.org/10.1016/j.pmcj.2011.09.004. URL <http://www.sciencedirect.com/science/article/pii/S1574119211001246>
- [70] P. Sapiezynski, A. Stopczynski, D. D. Lassen, S. Lehmann, Interaction data from the copenhagen networks study, *Scientific Data* 6 (1) (2019) 315. doi:10.1038/s41597-019-0325-x. URL <https://doi.org/10.1038/s41597-019-0325-x>
- [71] Y. Vaizman, K. Ellis, G. Lanckriet, Recognizing detailed human context in the wild from smartphones and smartwatches, *IEEE Pervasive Computing* 16 (4) (2017) 62–74.
- [72] M. G. Campana, F. Delmastro, Mydigitalfootprint: An extensive context dataset for pervasive computing *Pervasive and Mobile Computing* 70 (2021) 101309. doi:https://doi.org/10.1016/j.pmcj.2020.101309. URL <https://www.sciencedirect.com/science/article/pii/S1574119220301383>
- [73] R. Rawassizadeh, M. Tomitsch, K. Wac, A. M. Tjoa, Ubiqlog: a generic mobile phone-based life-log framework, *Personal and ubiquitous computing* 17 (4) (2013) 621–637.
- [74] R. Rawassizadeh, E. Momeni, C. Dobbins, P. Mirza-Babaei, R. Rahnamoun, Lesson learned from collecting quantified self information via mobile and wearable devices, *Journal of Sensor and Actuator Networks* 4 (4) (2015) 315–335. doi:10.3390/jsan4040315. URL <https://www.mdpi.com/2224-2708/4/4/315>
- [75] W.-X. Zhou, D. Sornette, R. A. Hill, R. I. Dunbar, Discrete hierarchical organization of social group sizes, *Proceedings of the Royal Society B: Biological Sciences* 272 (1561) (2005) 439–444.

- [76] R. Dunbar, V. Arnaboldi, M. Conti, A. Passarella, The structure of online social networks mirrors those in the offline world, *Social Networks* 43 (2015) 39 – 47. doi:<https://doi.org/10.1016/j.socnet.2015.04.005>. URL <http://www.sciencedirect.com/science/article/pii/S0378873315000313>
- [77] D. Comaniciu, P. Meer, Mean shift: a robust approach toward feature space analysis, *IEEE Transactions on Pattern Analysis and Machine Intelligence* 24 (5) (2002) 603–619.
- [78] R. Sibson, SLINK: An optimally efficient algorithm for the single-link cluster method, *The Computer Journal* 16 (1) (1973) 30–34. arXiv:<https://academic.oup.com/comjnl/article-pdf/16/1/30/1196082/160030.pdf>, doi:10.1093/comjnl/16.1.30. URL <https://doi.org/10.1093/comjnl/16.1.30>
- [79] A. Baldominos, A. Cervantes, Y. Saez, P. Isasi, A comparison of machine learning and deep learning techniques for activity recognition using mobile devices, *Sensors* 19 (3) (2019). doi:10.3390/s19030521. URL <https://www.mdpi.com/1424-8220/19/3/521>
- [80] D. P. Kingma, J. Ba, Adam: A method for stochastic optimization, arXiv preprint arXiv:1412.6980 (2014).
- [81] S. Ioffe, C. Szegedy, Batch normalization: Accelerating deep network training by reducing internal covariate shift, in: F. Bach, D. Blei (Eds.), *Proceedings of the 32nd International Conference on Machine Learning*, Vol. 37 of *Proceedings of Machine Learning Research*, PMLR, Lille, France, 2015, pp. 448–456. URL <http://proceedings.mlr.press/v37/ioffe15.html>
- [82] P. Baldi, P. J. Sadowski, Understanding dropout, *Advances in neural information processing systems* 26 (2013) 2814–2822.
- [83] B. Krawczyk, Learning from imbalanced data: open challenges and future directions, *Progress in Artificial Intelligence* 5 (4) (2016) 221–232. doi:10.1007/s13748-016-0094-0. URL <https://doi.org/10.1007/s13748-016-0094-0>
- [84] A. P. Bradley, The use of the area under the roc curve in the evaluation of machine learning algorithms, *Pattern Recognition* 30 (7) (1997) 1145–1159. doi:[https://doi.org/10.1016/S0031-3203\(96\)00142-2](https://doi.org/10.1016/S0031-3203(96)00142-2). URL <https://www.sciencedirect.com/science/article/pii/S0031320396001422>
- [85] J. Hu, H. Yang, M. R. Lyu, I. King, A. Man-Cho So, Online non-linear auc maximization for imbalanced data sets, *IEEE Transactions on Neural Networks and Learning Systems* 29 (4) (2018) 882–895. doi:10.1109/TNNLS.2016.2610465.

- [86] T. Fawcett, An introduction to roc analysis, *Pattern Recognition Letters* 27 (8) (2006) 861–874, rOC Analysis in Pattern Recognition. doi:<https://doi.org/10.1016/j.patrec.2005.10.010>. URL <https://www.sciencedirect.com/science/article/pii/S016786550500303X>
- [87] F. Pedregosa, G. Varoquaux, A. Gramfort, V. Michel, B. Thirion, O. Grisel, M. Blondel, P. Prettenhofer, R. Weiss, V. Dubourg, J. Vanderplas, A. Passos, D. Cournapeau, M. Brucher, M. Perrot, E. Duchesnay, Scikit-learn: Machine learning in Python, *Journal of Machine Learning Research* 12 (2011) 2825–2830.
- [88] T. O’Malley, E. Bursztein, J. Long, F. Chollet, H. Jin, L. Invernizzi, et al., Kerastuner, <https://github.com/keras-team/keras-tuner> (2019).
- [89] L. Li, K. Jamieson, G. DeSalvo, A. Rostamizadeh, A. Talwalkar, Hyperband: A novel bandit-based approach to hyperparameter optimization, *The Journal of Machine Learning Research* 18 (1) (2017) 6765–6816.

